ADVANCED ENERGY MATERIALS
www.advenergymat.de

Stretchable Supercapacitors as Emergent Energy Storage Units for Health Monitoring Bioelectronics

Xue Chen, Nicolo Simone Villa, Yanfeng Zhuang, Linzhe Chen, Tianfu Wang, Zida Li, and Tiantian Kong**

Emerging health monitoring bioelectronics require energy storage units with improved stretchability, biocompatibility, and self-charging capability. Stretchable supercapacitors hold great potential for such systems due to their superior specific capacitances, power densities, and tissue-conforming properties, as compared to both batteries and conventional capacitors. Despite the rapid progress that has been made in supercapacitor research, practical applications in health monitoring bioelectronics have yet to be achieved, requiring innovations in materials, device configurations, and fabrications tailored for such applications. In this review, the progress in stretchable supercapacitor-powered health monitoring bioelectronics is summarized and the required specifications of supercapacitors for different types of application settings with varying demands on biocompatibility are discussed, including nontouching wearables, skin-touching wearables, skin-conforming wearables, and implantables. The perspective of this review is then broadened to focus on integration of stretchable supercapacitors in bioelectronics and aspects of energy harvesting and sensing. Finally further insights on the existing challenges in this developing field and potential solutions are provided.

1. Introduction

Consumer electronics has experienced tremendous development in the past a few decades, mainly attributed to the steady innovation in semiconductor fabrication technology. These innovations enabled constant miniaturization in device sizes, reduction in the power consumption, and integration of functionality, making electronic devices more affordable with improved user experience. Consequently, consumer electronics has found ubiquitous applications in daily life, including entertainment, communications, and home–office activities, with the field of applications being expanded as the technology further develops. In particular, as the technologies of consumer electronics, high-volume data analysis, and medical science converge, much effort has been devoted to exploring the applications of electronic devices in health monitoring in recent years.[1,2]

Health monitoring devices offer the opportunity to continuously collect data on health conditions, including vital signs,[3,4] body motions,[5] metabolism status,[6] and even biomarker levels.[7] These data can be analyzed in real time, providing close monitoring of the health conditions and in-time suggestions on interventions if necessary. Given the aging problem around the globe, especially in developed countries, and the resultant increasing cost on healthcare, health monitoring devices can drastically reduce the burden on ambulatory care as well as inpatient care by providing health condition alert and early diagnosis.[2]

Health monitoring devices typically comprise three parts, namely sensing unit, data transmission unit, and power unit.[4] Sensing unit senses the input parameters, such as pulse, blood pressure, and temperature, and then converts the input into electrical signals as output, which are preprocessed and transmitted by the data transmission unit to another device, such as cloud or cell phone, for further analysis and interpretation. Both the sensing and data transmitting process require the powering from a battery or alike. Compared to other electronic devices, health monitoring devices have special requirements on the power unit. First, the power unit as well as the device itself need to have good stretchability, to ensure conformable contact on the body and consistent sensing performance. Second, since the device is likely to be in contact with bodily parts, the power unit and the device need to possess good biocompatibility to avoid unwanted immune response and other adverse effect. Lastly, for power unit in particular, given that oftentimes health monitoring devices have only minute power consumption, it is amenable to incorporate an energy harvesting unit to charge the power unit with energy from intermittent body motion, which requires a fast charging rate.[8]

Dr. X. Chen, N. S. Villa, Y. Zhuang, L. Chen, Prof. T. Wang, Dr. Z. Li, Dr. T. Kong
Guangdong Key Laboratory for Biomedical Measurements and Ultrasound Imaging
Department of Biomedical Engineering
School of Medicine
Shenzhen University
Shenzhen 518060, China
E-mail: zidali@szu.edu.cn; ttkong@szu.edu.cn
Dr. X. Chen
School of Mechanical and Electrical Engineering
Guilin University of Electronic Technology
No.1 Jinji Road, Guilin 541004, China
The ORCID identification number(s) for the author(s) of this article can be found under https://doi.org/10.1002/aenm.201902769.

DOI: 10.1002/aenm.201902769

Rechargeable batteries, especially lithium ion battery (LIB), have been most widely used in consumer electronic devices as well as health monitoring devices. LIB stores energy electrochemically through faradaic reactions and thus possesses high energy density.[9] Despite that, LIB has a few drawbacks including slow charging–discharging rate and suboptimal cycle stability. In addition, there has been safety concern about LIB, such as explosion and toxicity. In the context of health monitoring, compromised safety could be a deal-breaker and the slow charging rate also limits the harvest of energy from body motion.

As a potential alternative to battery, supercapacitors have been under intensive investigations in recent years. Conventional capacitors store energy in the electric field generated by two oppositely placed electrodes, which generally have high power density and good cycle stability but low energy density. In contrast, supercapacitor uses ion-rich liquid or hydrogel as the electrolyte and generates electrostatic double-layer capacitance and/or electrochemical pseudocapacitance on the electrodes, which greatly increases the energy density. With advantages of both capacitors and batteries, supercapacitors hold the potential to serve as the next generation power storage units for bioelectronics.

Stretchable supercapacitors are supercapacitors made from soft and stretchable materials. Their elastic modulus is closer to skin and tissues than rigid supercapacitors, which could potentially reduce the possibility of immune responses.[10] Moreover, they can accommodate movements of substrates such as clothes, skin, and soft tissue, owing to the robust performance under various deformations. These attributes make stretchable supercapacitors promising for health monitoring bioelectronics. Efforts have been devoted to developing stretchable supercapacitors with merits of good biocompatibility, stretchability, and energy storage performance, by exploring novel materials for electrodes and electrolytes, supercapacitor configurations and fabrications, and self-charging mechanisms.

A few reviews have thoroughly summarized the research status of flexible supercapacitors, with focus on the materials and/or architecture.[11–15] For example, Dubal et al.[11] introduced latest advances in flexible solid-state supercapacitors and provided new insights on mechanisms, emerging electrode materials, flexible gel electrolytes, and novel device designs. Zhao et al.[15] discussed the recent progresses on fabrication strategies of flexible supercapacitors for wearable devices. However, summaries on the specific applications of stretchable supercapacitors in health monitoring is largely inadequate. Such summaries would place stretchable supercapacitors in this practical context and prescribe an application-oriented requirement on the design of stretchable supercapacitor, which is essential for bridging the gap between academic exploration and practical applications.

In this review, we consolidate the recent applications of stretchable supercapacitors as powering units in health monitoring devices and reflect on the impact of biocompatibility, stretchability, and performance of stretchable supercapacitors in different application context (**Figure 1**). We start by introducing the basics of stretchable supercapacitors, including mechanisms, materials, and configuration designs that are applicable for bioelectronics. We then present the overview of the applications of different categories, namely nontouching wearables, skin-touching wearables, skin-conforming wearables, and implantables, with increasing biocompatibility requirements. In addition, we discuss specific concerns of the

Xue Chen is currently a postdoctoral fellow at Shenzhen University. She received her Master's degree and Ph.D. in the Institute of Mechanics, Chinese Academy of Sciences in 2014 and 2017, respectively. Then, she worked as an assistant professor at Guilin University of Electronic Technology. Since January 2018, she worked as a joint postdoctoral fellow in Dr. Tiantian Kong's and Dr. Zhou Liu's group at Shenzhen University. Her research interests include microfluidics, 3D printing, colloids and electrohydrodynamics.

Zida Li is an Assistant Professor in Biomedical Engineering at Shenzhen University. He received his B.S. in Mechanical Engineering from the University of Science and Technology of China and then worked as a Research Assistant at the University of Hong Kong. He received his Ph.D. from the University of Michigan, Ann Arbor, working on the nexus of micro/nanoengineering and biology. His research interests include flexible strain sensors, microfluidics, mechanobiology, and single cell technology.

Tiantian Kong is currently an associate professor at Shenzhen University. She received her master degree and PhD in Mechanical Engineering from University of Hong Kong in 2009 and 2013, respectively. Between 2013 and 2014, she worked as a joint postdoctoral fellow in Prof. Liqiu Wang and Dr. Ho Cheung Shum's group at the University of Hong Kong. She started her academic career in 2015 in the Department of Biomedical Engineering of Shenzhen University as an assistant professor. In 2018, she was promoted to associate professor. Her current scientific interests include microfluidics, microscale flows, soft bioelectronics and bioprinting.

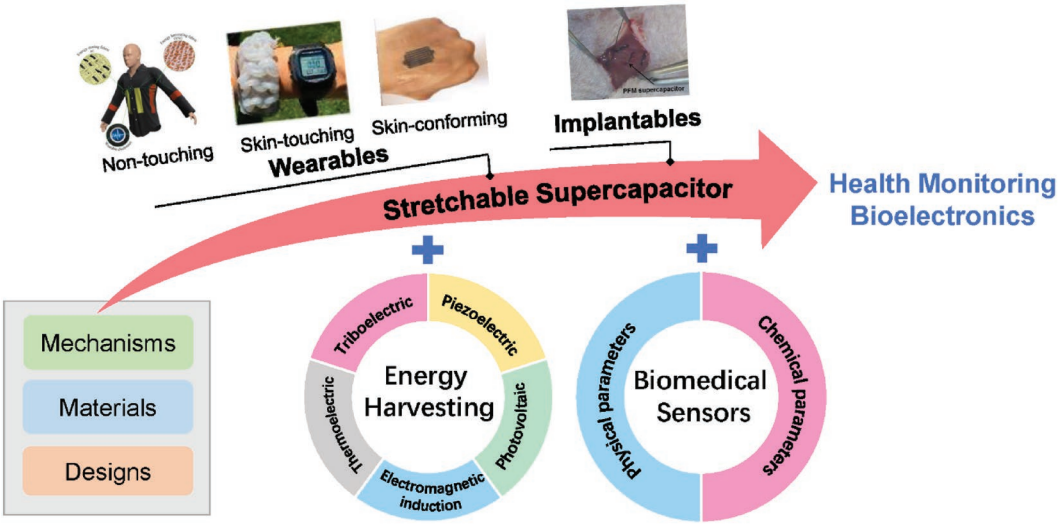

Figure 1. A graphic overview of this review. Section 2 introduces the basics of stretchable supercapacitors, including mechanisms, materials of electrodes and electrolytes, and designs of 1D, 2D, and 3D configurations and fabrications. Section 3 discusses the specific applications that were powered by stretchable supercapacitors, including nontouching wearables, skin-touching wearables, skin-conforming wearables, and implantables. Section 4 presents additional units other than stretchable supercapacitors in health monitoring bioelectronics, including energy harvesting unit and sensor unit. The four photographs on top reproduced with permission.[199,219,231,236] Copyright 2015, WILEY-VCH Verlag GmbH & Co. KGaA, Weinheim, 2017, American Chemical Society, 2016, WILEY-VCH Verlag GmbH & Co. KGaA, Weinheim, and 2018, Elsevier Ltd., respectively.

integration of stretchable supercapacitors in health monitoring devices, including self-charging and target sensing. Finally, we conclude the review with comments on the existing challenges and potential solutions.

2. Basics of Stretchable Supercapacitors

To monitor health conditions via human activities, wearable and implantable supercapacitors should comply to the associated deformations. As such, they need to be flexible for bending and twisting, even stretchable to endure sudden and frequent stretch-and-release cycles, while still possessing sufficient energy density, power density, and cycle stability at these deformations. These desirable merits put forward high requests to the physical and chemical properties of both the electrodes and electrolytes, as well as the configuration designs. To assist the understanding of these merits in application contexts, this section provides an overview on the fundamentals of stretchable supercapacitors, including mechanisms, materials, and device designs, in order to guide the route toward the recent advances in stretchable bioelectronics with improved performances and stretching reliability.

2.1. Mechanisms

Though the detailed charge-storage mechanism of supercapacitors remains to be elucidated, it is generally agreed that there exist mainly two types of mechanisms, namely electrical double-layer capacitance (EDLC) and pseudocapacitance,[16] as shown in **Figure 2**. In EDLC, the charge is stored in the Helmholtz double layer at the interface between the electrode and electrolyte. As the thickness of the Helmholtz double layer is typically 0.6–1 nm, which is much smaller than that of conventional capacitors, a much higher capacitance is achieved. Given that EDLC relies on the electrostatic charges accumulated on the surface of the electrodes, to boost the energy density of EDLC, a straightforward strategy would be increasing the specific surface area (SSA). Indeed, in early studies, porous carbon materials, such as carbon nanotubes, graphene, and other activated carbons, were commonly used as the electrode materials. Their high porosity generally resulted in good performance.[17]

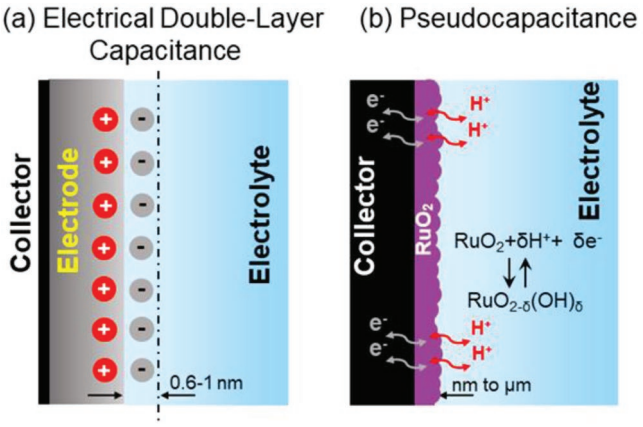

Figure 2. Schematics showing two different mechanims of supercapacitors, namely a) electrical double-layer capacitance (EDLC) and b) pseudocapacitance. In EDLC, the charge is stored in the Helmholtz double layer at the interface between the electrode and electrolyte. In pseudocapacitance, the charge is electrochemically stored through faradaic charge transfer between the electrode and electrolyte through processes such as redox reaction, as indicated by the chemical equation. Reproduced with permission.[25] Copyright 2011, Cambridge University Press.

However, it was later found that, as the SSA was increased by adjusting pore sizes, the supercapacitor performance did not improve linearly. When the pore size was decreased to below 1 nm, the capacitance increased abruptly.[18–20] It was proposed that the increase of the capacitance at sub-nanometer pores was attributed to the exponential screening of the electrostatic interaction in the pores together with the image-charge ionic attraction at the pore surfaces.[21] When accessing small nanopores, ions lost part of their solvation shells in order to fit inside.[22] Based on the density functional theory and molecular dynamics study, it was found that the degree of confinement of the ions, which increases the desolvation process, has the highest efficiency at a pore size of 0.7 nm. Increasing the pore size to multiple ion diameters resulted in a loss of capacitance.[23,24]

The main issue of EDLC is the relatively low energy density. In contrast, the typical energy density of pseudocapacitance can be 100 times higher than that of EDLC, which is beneficial for energy storage.[24] In pseudocapacitance, the charge is electrochemically stored through faradaic charge transfer between the electrode and electrolyte, mainly accomplished through three processes, namely underpotential deposition, redox reaction, and intercalation.[25] In contrast to batteries, the faradaic charge transfer does not alter the atomic structure of the electrodes, making the charge–discharge rate much higher.[11,26]

Stretchable supercapacitors include both EDLC and pseudocapacitor. A few metrics have been commonly used to assess the performance of stretchable supercapacitors in health monitoring applications, including stretchability, volumetric or areal capacitance, energy density, power density, and cyclic voltammetry stability. Stretchability is defined as the capability of the device to be stretched. Energy density describes the amount of energy that can be stored per unit volume or area. Power density describes the rate to deliver the energy stored in the supercapacitor to an external load per unit volume or area. Cyclic voltammetry results represent the cycle stability of the supercapacitors.

2.2. Materials

Materials dictate the functionality and performance of the resultant supercapacitors. To develop stretchable supercapacitors, the materials of both the electrodes and electrolytes need to withstand high strain without significant compromise on the electrochemical properties. To this end, two major strategies have been adopted to develop materials with stretchability: exploring novel materials that are inherently stretchable and depositing conductive materials of wavy, buckled, or island-bridge configurations on stretchable substrates to realize high stretchability.[27,28]

2.2.1. Electrodes

Electrodes are normally arranged in either symmetric fashion, where both electrodes are made from the same material, or asymmetric fashion, where cathode and anode adopt different materials.[29–31] In symmetric configuration, the voltage window is normally lower than 1 V. In contrast, asymmetric supercapacitors typically use a pseudocapacitive material on the cathode and a non-faradaic material on the anode, retaining the advantages of both EDLC and pseudocapacitor, thus exhibiting a potential window up to 2 V.[32,33]

Innovation has been made in the development of various electrode materials,[12,14] as shown in **Figure 3**. Carbon-based materials (CBs), metal oxide (MOs), and conductive polymers (CPs)

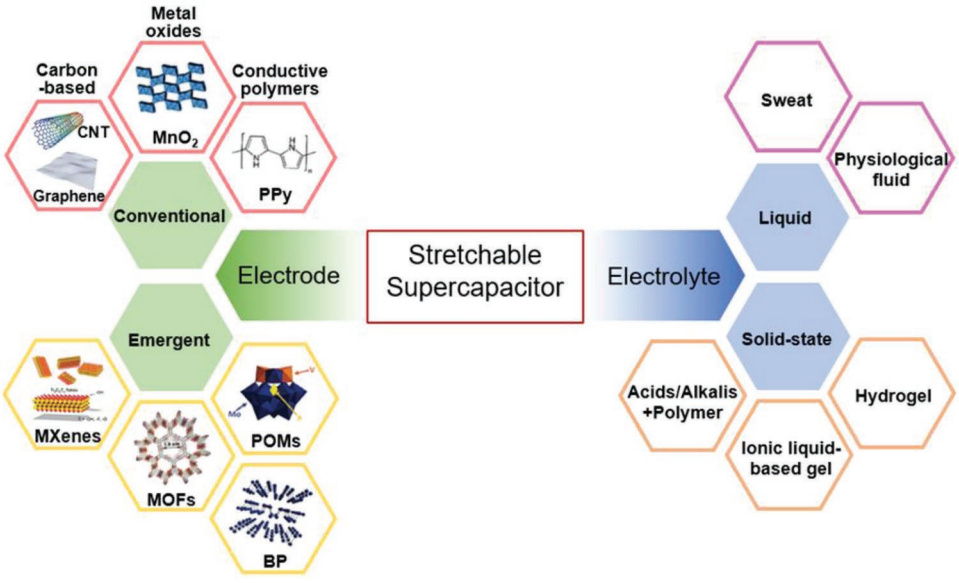

Figure 3. An overview of the electrode and electrolyte materials utilized in stretchable supercapacitors for health monitoring devices. Electrode materials include conventional materials (e.g., carbon-based, metal oxide, and conductive polymers) and emergent materials (e.g., MXenes, POMs, MOFs, and BP). For electrolyte materials, liquid electrolyte such as sweat and other body fluids have been used in implantables and solid-state electrolytes including acids/alkalis with polymers, ionic liquid-based gel, and hydrogel have been used in wearables. Molecule schematics reproduced with permission.[11] Copyright 2018, The Royal Society of Chemistry.

are among the most studied.[33] With the advances in materials science and engineering, many emergent materials, such as MXenes, polyoxometalates (POMs), metal-organic frameworks (MOFs), and black phosphorus (BP), have shown superior electrochemical performance.[11,26] In this section, we introduce different types of electrode materials and their characteristics.

Conventional Materials: Carbon-based materials are widely used in stretchable electrode designs, mainly due to their low cost, easy accessibility, and high SSA. For instance, activated carbons are usually obtained by carbonizing charcoal, resulting in high degree of microporosity and thus high SSA. Many commercial stretchable supercapacitors adopted activated carbon as electrodes, exhibiting high specific capacitance up to 0.51 F cm^{-2} and little capacitance loss upon 50% stretching.[34] Activated carbon powder can also be mixed with other carbon materials such as carbon black to form composite electrode materials. Graphene, a 2D carbon material, has been widely applied as prominent stretchable electrodes for stretchable supercapacitors, owing to their large surface area, high electrical/ionic conductivity, and mechanical properties.[35–37] Its derivative, graphene oxide (GO), is a major precursor for mass production of graphene in its reduced form, reduced GO (rGO). For example, multilayer graphene sheets were deposited on wrinkle-structured PDMS substrate as stretchable electrodes, resulting in transparent supercapacitors with a stretchability of 40%.[38] An all-graphene core–sheath fiber was designed for a spring-like stretchable supercapacitor, which demonstrated a large stretchability of 200%.[39] Carbon nanotube (CNT) has been shown as an excellent candidate for the electrode in stretchable supercapacitors, given their excellent electrical properties, high stability, and high aspect ratio.[40,41] For example, researchers fabricated CNT/graphene/PANI composite as the electrode of a stretchable supercapacitor.[41] The performance of the resultant supercapacitor was stable under 180% stretch with energy densities of 36.3 to 29.4 μWh cm^{-2} and power densities of 0.17 to 5 mW cm^{-2} at current densities of 0.1 to 3 mA.

Metal oxides have been widely used as electrode materials for pseudocapacitors. Commonly used metal oxides include RuO_2, MnO_2, SnO_2, V_2O_5, MoO_x, Co_2O_3, and NiO, with RuO_2 and MnO_2 being the most utilized in stretchable electrodes. Metal oxides can store charge through fast, reversible surface redox reactions, but they typically have suboptimal cycling stability and relatively low capacitance. To improve the overall performances, metal oxides are often combined with carbon materials or conductive polymers to construct stretchable electrodes.[42,43] For example, researchers deposited MnO_2 and Fe_2O_3 on the CNT films to serve as positive and negative electrodes, respectively.[44] The asymmetric stretchable supercapacitor exhibited excellent electrochemical performance and a high stretchability of 100%.

Conductive polymers are inherently stretchable and pseudocapacitive. Frequently used conductive polymers include polypyrrole (PPy), poly(3,4-ethylenedioxythiophene) (PEDOT), poly(3-methylthiophene) (P3MT), and polyaniline (PANI).[45–47] Their conductivity is much lower than carbon materials and metal oxides. Efforts have been devoted to enhancing the conductivity of conductive polymers, for instance, by mixing them with carbon materials. For example, gold nanoparticle/CNT/poly(acrylamide) hydrogel incorporated with PPy was synthesized as electrodes to assemble a stretchable, self-healing supercapacitor.[48] The resultant supercapacitor exhibited an areal-capacitance of 885 mF cm^{-2}, an energy density of 123 μWh cm^{-2}, and a stretchability as high as 800%.

Emergent Materials: Emergent materials could potentially bring in efficient charge transfer mechanisms and revolutionize the field of stretchable supercapacitors. The emergent materials, include MXenes, MOFs, POMs, and BP, have shown superior performance as electrodes. As such, the application potential of these new materials in stretchable supercapacitor is worth exploring. Here we briefly introduce the studies involving these materials for stretchable bioelectronics. A detailed overview can be found in another review paper.[26]

MXenes are a new family of 2D materials with outstanding electrochemical and mechanical properties, making them beneficial for energy storage devices.[49–53] MXenes are usually found in a $M_{n+1}X_nT_x$ phase where M is a transition metal, X is either carbon or nitrogen, and T represents surface termination. They have superior intrinsic electrical conductivity and abundant surface-active groups, which is favorable for fast charge/discharge process. The charge storage of MXenes is pseudocapacitive, and the layered structure of MXenes is considered to prevent dense stacking, resulting in porous structures that are favorable for ion transport.[54,55] To further facilitate ion transport of multilayered MXenes, introducing molecular spacers was found to improve transport abilities among layers though at the cost of the volumetric capacitance.[56]

MOFs are promising electrode materials due to their high porosity, open pore framework, and chemical tunability.[57] However, MOFs have poor conductivity, which limits their practical applications. A common strategy is to add conductive materials to form composite electrodes,[58] though additive-free MOF-based supercapacitors have also been reported with relatively disadvantageous electrochemical properties.[59] For instance, core–shell ZnO@ZIF-8 on carbon cloth with PANI coating was synthesized and used to fabricate flexible supercapacitors with high areal capacitance.[60] Nevertheless, a subgroup of MOFs was found to possess exceptional charge transport capabilities due to their π–π stacking between the 2D MOFs layers. These MOFs have been applied as stretchable electrodes for supercapacitors.[61]

POMs are clusters of early transition-metal anionic with great redox and electronic transfer abilities, also known as "electron sponge."[57,62] POMs consist of 3D frameworks including oxygen and early transition metals present at their high oxidation states. For this reason, POMs usually have good oxidative abilities and their reductive products possess reductive abilities, making them suitable to achieve high capacitance for energy storage systems. For example, researchers used PMo_{12} to initiate PPy polymerization and simultaneously reduce GO to develop an electrode material.[62] The resultant supercapacitor exhibited an areal-capacitance of 2.61 mF cm^{-2} at a current density of 150 mA cm^{-2}, which was much higher than the analog PPy/rGO without the addition of the POM due to the pseudocapacitive properties of PMo_{12}.

2D BP is a p-type direct bandgap semiconductor with unique optoelectronic and electrical properties.[63] BP has a layered lamellar structure of P atoms with highly spaced (5.3 Å) layers bonded by Van der Waals interactions. The use of BP in stretchable supercapacitor is growing and several reports have shown successful implementations, especially in combination with

carbon-based materials or conductive polymers.[64,65] For example, researchers developed a BP/CNT hybrid material by chemically bridging CNT and BP by C—P bond. A microfluidic spinning technique was used to assemble the resultant material into a supercapacitor electrode.[66] The as-fabricated supercapacitors exhibited excellent stretchability, rate capability, and cycle stability.

2.2.2. Electrolytes

Stretchable electrolyte is another key component to develop supercapacitors with high stretchability and good electrochemical performance. Ideally, stretchable electrolyte should have high ionic concentration, good conductivity, high electrochemical stability, good biocompatibility, and good stretchability.[67–69] Commonly used electrolytes are either liquid electrolytes or solid-state electrolytes.[70–73] Aqueous-based, organic solvent-based, and ionic liquids are typical liquid electrolytes in commercial applications. For implantable applications, sweat and other physiological fluids, such as blood, have been used as liquid electrolytes.[72,74,75] A common issue with liquid electrolytes in health monitoring context is the risk of leakage, leading to the sought of solid-state stretchable electrolytes with highly mobile ions, low cost packaging, and good mechanical stability. To this end, three main types of solid-state electrolytes have been utilized, including gel electrolytes, ceramic electrolytes, and polyelectrolyte, with gel electrolytes being the most studied given their good stretchability and biocompatibility.[11]

Gel electrolytes, like H_3PO_4/PVA and H_2SO_4/PVA, are commonly used for most of the stretchable supercapacitors, given their good ion transportation and mechanical stretchability.[42,76] For example, a highly stretchable H_3PO_4/PVA polymer electrolyte coupled with electrode of conductive polymer, namely polypyrrole, was reported, which showed an excellent fracture strain at 410% elongation and a high conductivity of 3.4×10^{-3} S cm^{-1}.[77] This supercapacitor also exhibited good capacitance retention of 94.5% at 30% strain, and can retain 81% after 1000 stretch/release cycles. Thereafter, various polymer matrixes have been utilized, including PMMA, PAA, PEO, PAM, and PVDF,[66,78–80] and electrolytic salts such as KOH, LiCl, and $LiClO_4$ have also shown utility as the ion source.[81–83] However, strong acids/alkalis in the gel electrolyte may pose safety issues for implanted bioelectronic devices. To overcome this problem, a strategy was proposed to replace acid with ionic liquids as additives in gel electrolytes. Using ionic liquid-based gel electrolyte, stretchable supercapacitors with a high ion conductivity and a wider potential window up to 2.5 V was achieved.[84] Consequently, an increased cell voltage and maximum specific energy density was achieved. Owing to the superior properties such as high thermal stability, low vapor pressure, and nonflammability, ionic liquid-based gel has been widely used in energy storage devices.[85–87]

Advances in hydrogel engineering also offer the opportunity to develop versatile gel electrolytes with additional features such as healability, biocompatibility, and transparency,[88–92] which can be valuable in some health monitoring context. Recently, a polyacrylic acid (PAA)-based stretchable electrolyte, which was dually crosslinked by hydrogen bonding and VSNPs-PAA, was synthesized to develop a self-healable supercapacitor.[93] The supercapacitor could be stretched with up to 600% strain and retain the capacitance when subjected to 20 breaking cycles. In the meanwhile, it was able to recover from the break at room temperature without obvious capacitance degeneration. Recently, a highly elastic and reversibly stretchable supercapacitor using a double network hydrogel electrolyte and PPy electrode was also developed.[94] Such hydrogel possessed excellent mechanical properties, with a stretchability of 500% and good reversibility from strain residue.

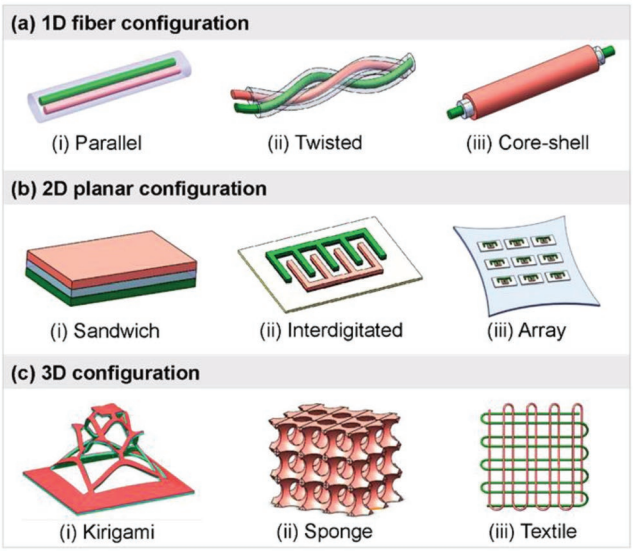

Figure 4. Schematic illustration of three typical configurations of supercapacitors: a) 1D fiber configuration (e.g., parallel, twisted, and core–shell fibers), b) 2D planar configuration (e.g., sandwich, interdigitated, and arrays on chip), and c) 3D configuration (e.g., kirigami, sponge, and textile substrate).

2.3. Device Configurations and Fabrication Methods

Device configuration affects the performance and dimensions of stretchable supercapacitors. Recently, considerable efforts have been devoted to developing novel architecture designs of stretchable supercapacitors, which can be divided into 1D fiber-like (parallel, twisted, and core–shell fibers), 2D planar (sandwich, interdigitated, and arrays on chip), and 3D configurations (kirigami, porous sponge, and textile substrate), as shown in **Figure 4**. The realization of these state-of-the-art architectures relies on the employment of sophisticated fabrication techniques, such as spinning, photolithography, etching, templating, and deposition approaches. In this section, we introduce several configurations and their representative fabrication strategies that were aimed to improve the overall performance, with highlight on the potentials of these stretchable supercapacitors for biomedical applications.

2.3.1. 1D Fiber Design

1D Fiber Configuration: The 1D fiber-like stretchable supercapacitors emerged and developed rapidly in the past a few years,[95–97] owing to their lightweight, stretchability, and knittability.

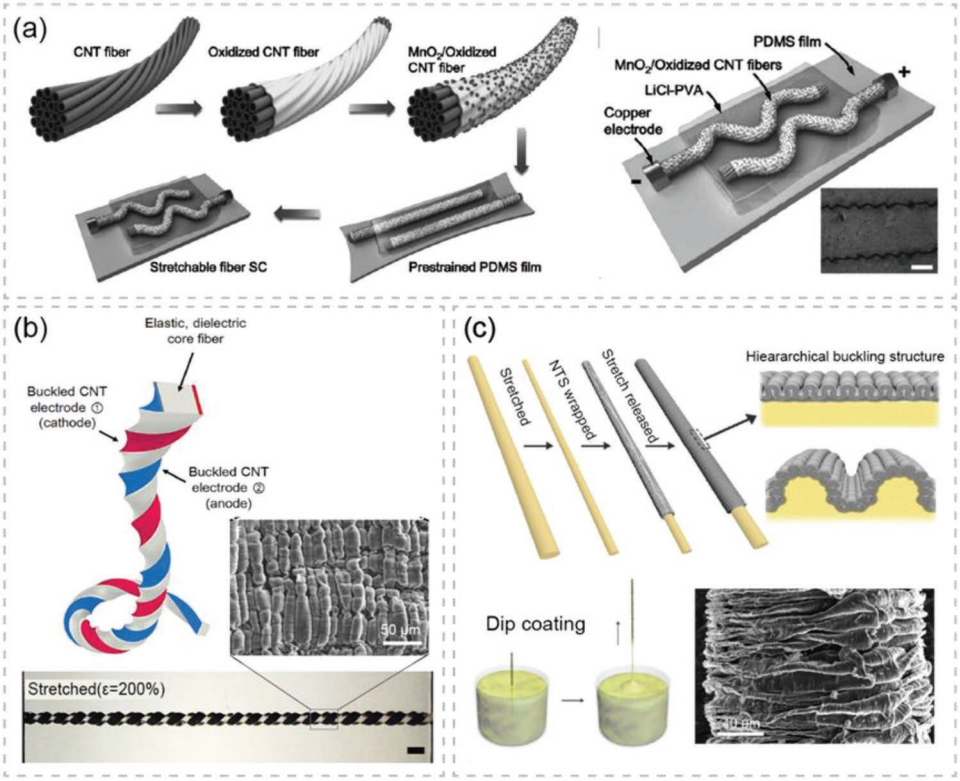

Figure 5. Schematic illustration of novel designs of 1D stretchable fiber supercapacitors. a) Fabrication process of the stretchable fiber supercapacitors and the assembled parallel device. Reproduced with permission.[100] Copyright 2017, WILEY-VCH Verlag GmbH & Co. KGaA, Weinheim. b) Prestraining and twisting methods to design stretchable fiber supercapacitors with stretchability up to 200%. SEM image shows microscopic CNT buckled structures after strain relaxation. Reproduced with permission.[107] Copyright 2016, American Chemical Society. c) Fabrication process of stretchable core–shell fibers with hierarchically buckled structures. SEM image shows NTS_5@$fiber_{350}$ made from Pt-coated NTSs by fabrication strain of 900%. Reproduced with permission.[114] Copyright 2016, WILEY-VCH Verlag GmbH & Co. KGaA, Weinheim.

Fiber-like supercapacitors can be easily woven or knitted into textiles to integrate multifunctional wearable and implantable bioelectronics. Typically, 1D stretchable supercapacitors can be configured by stretchable fiber electrodes in arrangements such as parallel, twisted, and core–shell (Figure 4a).

A simple structure of the fiber-like stretchable supercapacitor is two fiber electrodes in parallel separated by a solid-state stretchable electrolyte,[98,99] as shown in Figure 4a-i. Many fiber electrodes are sufficiently flexible to be bended and twisted, but they cannot be stretched without compromising device integrity, which limited their applications in stretchable supercapacitors. To address that, a helical or spring-like configuration by wrapping fiber electrodes around the stretchable substrate or electrolyte was developed, providing fiber electrodes with good stretchability. For instance, a parallel stretchable supercapacitor with MnO_2/oxidized CNT fiber electrode, PVA/LiCl gel electrolyte, and PDMS film was prepared in buckled pattern by prestrain method,[100] as shown in **Figure 5**a. It displayed a high volumetric energy density and capacitance of 6.3 mWh cm^{-3} and 409.4 F cm^{-3} at 0.75 A cm^{-3}, respectively, with no significant change in electrochemical properties under 40% applied strains. Gao's group fabricated a parallel-structured supercapacitor using PPy-decorated rGO and multiwalled carbon nanotubes (MWCNTs) composite fibers. The spring-like fibers were coated with stretchable polyurethane (PU) to ensure stretchability and self-healability. The resultant stretchable supercapacitor had 82.4% capacitance retention after stretch up to 100% and 54.2% capacitance retention after third healing.[89]

Fiber-like configuration can also be achieved by assembling twisted fiber electrodes with surface-coated electrolyte to form a stretchable supercapacitor (Figure 4aii). The stretchable twisted fiber electrodes can be prepared from intrinsically nonstretchable conductive materials.[101–106] A twisted fiber supercapacitor consisted of a dielectric core rubber sandwiched between functionalized buckled CNT electrodes was reported, as shown in Figure 5b. The as-fabricated stretchable fiber supercapacitor provided dual functions of high strain sensing (up to 200%) and electrical energy storage with retention of more than 95%.[107] To dramatically increase the stretchability of a fiber supercapacitor, ultrastretchable electrode with microscopically buckled and macroscopically coiled design was developed.[108] A core elastic rubber fiber was first coiled up with 4000 turns m^{-1} and stretching up to 1000%, and then CNT layers were wrapped on the pretwisted fiber. As a result, the synergistic structure was formed along the fiber during strain relaxation, providing the resultant supercapacitor with an elastic deformation up to 800% while retaining high charge storage capability. In particular, multifunctional stretchable supercapacitors are introduced, such as self-healable supercapacitors, electrochromic supercapacitors,[109] and shape-memory supercapacitors. For

instance, a self-healable stretchable supercapacitor based on twisted graphene oxide fibers was fabricated, which exhibited a capacitance retention of 82.4% after 100% stretching and 54.2% after three breaking/healing cycles.[101] In addition, a shape memory supercapacitor using NiTi memory alloy and MnO_2/PPy electrode was proposed.[110] The resultant supercapacitor could automatically recover its original shape and restore from deformations when heated over a triggering temperature. Supercapacitors with novel functionality, such as healability from physical damages, hold great potential in the design of biomedical devices with a long-life span.

Compared to twisted structure, the core–shell architecture (Figure 4aiii) has much larger effective area for ion storage and smaller size for packaging, providing stretchable supercapacitors with good electrochemical performance.[111,112] A highly stretchable supercapacitor was developed by wrapping aligned CNT sheets on a rubber fiber.[113] The as-designed core–shell fiber supercapacitor maintained a high specific capacitance of 18 F g^{-1} after being stretched with 75% strain for 100 charge/discharge cycles. To increase the stretchability, a superelastic fiber electrode was demonstrated by wrapping oriented CNT sheets on a prestretched rubber fiber, resulting in a core–shell structure,[114] as shown in Figure 5c. The resultant hierarchical buckled architecture was highly stretchable, which could tolerate strains up to 900%. It could be reversibly stretched over 72 times in the axial direction, with change in resistance being only 12%. Since the overall electrical conductivity decreases with increased core–to–shell volume ratio, downsizing the core diameter and length is beneficial for the improvement of the electrochemical performance of supercapacitors. Therefore, optimization of the stretchable fiber configurations is of great importance.

Fabrication Methods for 1D Fiber Design: Stretchable fiber supercapacitors can mainly be fabricated by two approaches: 1) coating conductive materials on stretchable fiber wires and 2) spinning conductive fiber electrodes from stretchable materials. Additional assistance methods, including pre-straining, self-twisting, and helix winding, usually endow fiber electrodes with improved electrochemical performances, stretchabilities, and multifunctionalities.[17,115] Among various coating methods, dip coating,[116] electrochemical deposition,[117] and hydrothermal synthesis[118] are the most frequently used in fiber supercapacitor fabrication. For instance, a wood rod was dipped into a molten rubber solution and withdrawn quickly,[114] and the generated polymer fiber was then pre-strained and wrapped with CNT layers (Figure 5c). A hydrothermal method had been used to synthesize rGO on the as-drawn conductive yarns.[119] Subsequently, the electrodeposition method was applied to coat MnO_2 nanosheet and PPy thin film on the fiber.

Spinning is one of the most used techniques for fabricating carbonaceous fibers as electrodes, with specific techniques including wet spinning,[120–122] dry spinning,[43,123,124] and microfluidic spinning.[125–127] Using microfluidics, well-dispersed GO and urea solution was injected into a coflowing microchannel, and N-doped graphene fibers with porous network and high electrical conductivity were obtained through in situ doping.[128] In microfluidic spinning, the diameter of the fibers can be tuned to optimize the performance of the resultant stretchable fiber supercapacitor by varying the injection rate, nozzle size, and solution rheology. Further efforts may be devoted to integrating fiber supercapacitors with textiles seamlessly and enduringly for practical applications.

2.3.2. 2D Planar Design

2D Planar Configuration: Conventional sandwich-type supercapacitors dominate practical applications in early researches. It contains two thin-film electrodes and solid-state electrolyte as the separator (Figure 4bi). The sandwich-type supercapacitors can be fabricated from stretchable materials or by adopting buckled/wavy designs using prestraining strategy.[12,13,38,129–131] For instance, a highly stretchable and omni-healable supercapacitor was constructed by sandwiching hydrogel electrodes and electrolytes, both of which could be healed from damages. The resultant sandwich-type supercapacitor exhibited a stretchability of 800%.[48] In another study, a new polyelectrolyte comprised of PAM–VSNPs was developed to fabricate wavy-pattern supercapacitor, resulting in a superstretchability of 1000% with 2.6-fold capacitance enhancement and compressibility of −50% with good retention of the initial performance.[132] The prestraining strategy was further extended to biaxial directions, providing stretchability along all in-plane directions.[35] As another instance, a hybrid nanomembrane supercapacitor was developed based on prestretched Ecoflex film,[133] as shown in **Figure 6**a. It exhibited a unique combination of high stretchability of 600% under biaxial strain, high capacitance of 77 F g^{-1}, and good reliability over 1000 stretch/ release cycles. Furthermore, a new design with aligned honeycomb-like structures of rGO/CNT electrode was proposed, exhibiting excellent retention ratio under different strains, namely over 91% retention under 100% uniaxial strain and 88% retention under 100% biaxial strain.[105]

Although stretchable supercapacitor with sandwich structure is easy to fabricate, it often imposes difficulties for system miniaturization. To address this problem, in-plane interdigitated supercapacitors[134,135] have been introduced (Figure 4bii). The interdigitated design provides a short distance for ion transport and a miniaturized size for packaging, which is favorable for developing small-sized energy storage systems. An interdigitated rGO-based stretchable microsupercapacitor with excellent specific capacitance and mechanical stability was demonstrated, which could be stretched up to 30% strain with no significant change in capacitance density.[136] However, if the planar interdigitated electrode is made from rigid materials, cracks may easily appear upon stretching. Thus, rigid conductive materials are typically made into wavy structure and then embedded in stretchable substrates to accommodate large strains. A hybrid MWCNT/PANI electrode was fabricated to form a fully stretchable microsupercapacitor, as shown in Figure 6b. Owing to the wavy shape of the electrodes, the resultant device presented a high areal specific capacitance of 44.13 mF cm^{-2} under stretching stations ranging from 5% to 40%.[137]

The energy density of a single supercapacitors is relatively low. A simple yet effective way to enhance their energy density is to connect several supercapacitors in arrays with a serpentine bridge-island connection (Figure 4b-iii). Stretchable microsupercapacitor arrays were fabricated with SWCNT electrode and ion-gel electrolyte, which were bonded by metallic serpentine bridge-island interconnections, as shown in Figure 6c.[138] As a

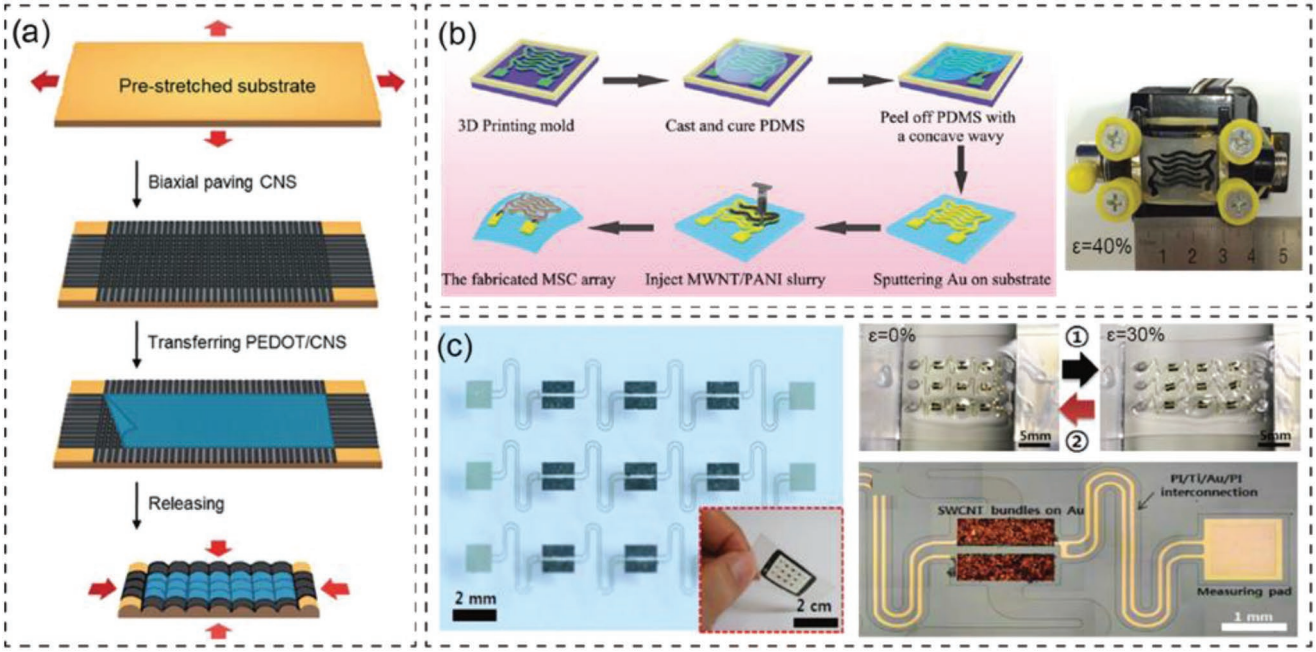

Figure 6. Schematic illustrations for 2D stretchable planar supercapacitors. a) Fabrication process of a stretchable PEDOT/CNS hybrid nanomembrane by biaxial prestraining and releasing method to form a wavy structure. Reproduced with permission.[133] Copyright 2016, The Royal Society of Chemistry. b) 3D printing method to fabricate the stretchable interdigitated supercapacitor with a buckled structure and the as-designed stretched object under 40% deformation. Reproduced with permission.[137] Copyright 2017, WILEY-VCH Verlag GmbH & Co. KGaA, Weinheim. c) Stretchable 2D planar supercapacitor arrays and the magnified optical image of a single supercapacitor with serpentine interconnections. Reproduced with permission.[138] Copyright 2013, American Chemical Society.

result, the device was stable over stretching up to 30% without noticeable degradation in capacitance and, it could power micro-LEDs under stretched states. However, solid metallic interconnects may break during a large deformation. An alternative method is using liquid metal to link the individual supercapacitors given the fluidic nature of liquid metal.[139] For example, a biaxially supercapacitor array embedded in stretchable Ecoflex substrate was introduced, where liquid metal was used to interconnect the supercapacitors.[140] It exhibited a high energy density of 25 mWh cm^{-3}, high power density of 32 W cm^{-3}, and stable electrochemical performance with negligible decrease in capacitance upon uniaxial and biaxial stretching up to 100% and 50%, respectively.

Fabrication Methods for2D Planar Design: 2D planar stretchable supercapacitors can be fabricated via sputtering,[141] spin/spray coating,[142] chemical vapor deposition (CVD),[36] 3D printing,[143,144] and layer by layer deposition.[145] Choosing suitable method is vital for the practical designs of planar supercapacitors. Sputtering, spin-coating, and spray-coating are commonly used to coat a thin film on flat substrates. Normally, sputtering is utilized in deposition of gold current collectors associated with micromasking technique. However, these coating techniques normally produce films with no internal porosity, which limits ion transport and consequently limits their applications. To overcome that, CVD methods were developed to fabricate thin film electrodes with high specific surface area, which could be extended to fabricate 2D layered materials. As an example, graphene sheets can be directly grew on nickel foil substrate by CVD method, and the resultant devices exhibited an exceptional frequency response and power density, owing to the large surface area of porous graphene electrode.[146] To further increase the mass loading and power density, layer-by-layer deposition was adopted, which allows the deposition of compact films that are permeable to ions. Free-standing β-$Ni(OH)_2$/graphene nanohybrids with unique layer-by-layer stacking characteristics were fabricated as electrodes, and the resultant supercapacitor exhibited extraordinary electrochemical performance and superior cycling stability.[82]

Micro/nanofabrication techniques, like etching, photolithography,[144] and laser writing,[147,148] can be used to pattern interdigitated architectures with high resolution. Etching is a powerful strategy with the capability of removing materials anisotropically to obtain microstructures with high aspect ratios, high fidelity, and high resolution.[71,149] For instance, dry etching, specifically reactive-ion etching (RIE),[71] was used to fabricate a well-defined 3D microstructure, and a MnO_2 thin film was then electrodeposited to form a micropattern electrode. In addition, by combining photolithography and a simple transfer method, freestanding rGO film on a gold-patterned photoresist bilayer was fabricated, and then MnO_2 was coated via electrochemical deposition on the rGO film to form electrodes.[150] The interdigitated electrodes with a spacing resolution of 50 μm led to a shortened diffusion path length, thus enhancing the ionic diffusion and resulting in increased total accessible electrochemical surface area. A laser direct writing technique was exploited to design interdigitated patterns with a lateral spatial resolution of 20 μm to achieve high power density.[151] As such, more than 100 microsupercapacitors could be readily generated on a single disk in less than 30 min, significantly improving the production efficiency. Recently, a microfluidic wet-etching method

has been utilized in the fabrication of in-plane supercapacitors. In the pioneering work by Xue et al.,[152] a thin layer of MnO_2 nanofiber film was first deposited by electrospinning, which was then transferred onto gel electrolyte and sputtered with an ITO layer. After that, microfluidic etching was used to fabricate interdigitated patterns in preformed microfluidic channels. This technique was simpler and more economically efficient than many traditional etching methods, making the microfluidic etching a promising method for electrode patterning.

2.3.3. 3D design

3D Configuration: Stretchable supercapacitors with 3D configurations can accommodate deformations omni-directionally, providing unique advantages compared to 1D and 2D configurations. Reported 3D configurations include kirigami-inspired structure,[153,154] 3D sponge structure,[155,156] and textile structure,[157] as shown in Figure 4c.

Kirigami-inspired structure (Figure 4c-i) is achieved by cutting paper-like supercapacitors into customizable 3D structures, and subsequently it can be stretched in arbitrary directions.[158–160] For example, a kirigami-inspired stretchable supercapacitor with arbitrary 3D structures (honeycomb-like, pyramid pop-up, and living-hinge) was designed based on stretchable MnO_2 nanowire electrode,[161] as shown in **Figure 7**a. The honeycomb-like architecture showed superior performance, with a specific capacitance of 227.2 mF cm^{-2} and stretchability of 500%. Meanwhile, nearly 98% capacitance could be maintained after 10 000 stretch-release cycles with 400% tensile strain. In addition, an origami-type stretchable supercapacitor was designed with a packed series connection fabricated by a unique patterning approach.[162] The proposed origami structure could increase energy and power simultaneously, and more importantly, it could accommodate stable deformation from –60% compression to 30% stretching. Using similar strategies, nonactive elastic substrates could be utilized to design the stretchable commercial electronics, such as watch strap[163] and integrated strain sensors.[161]

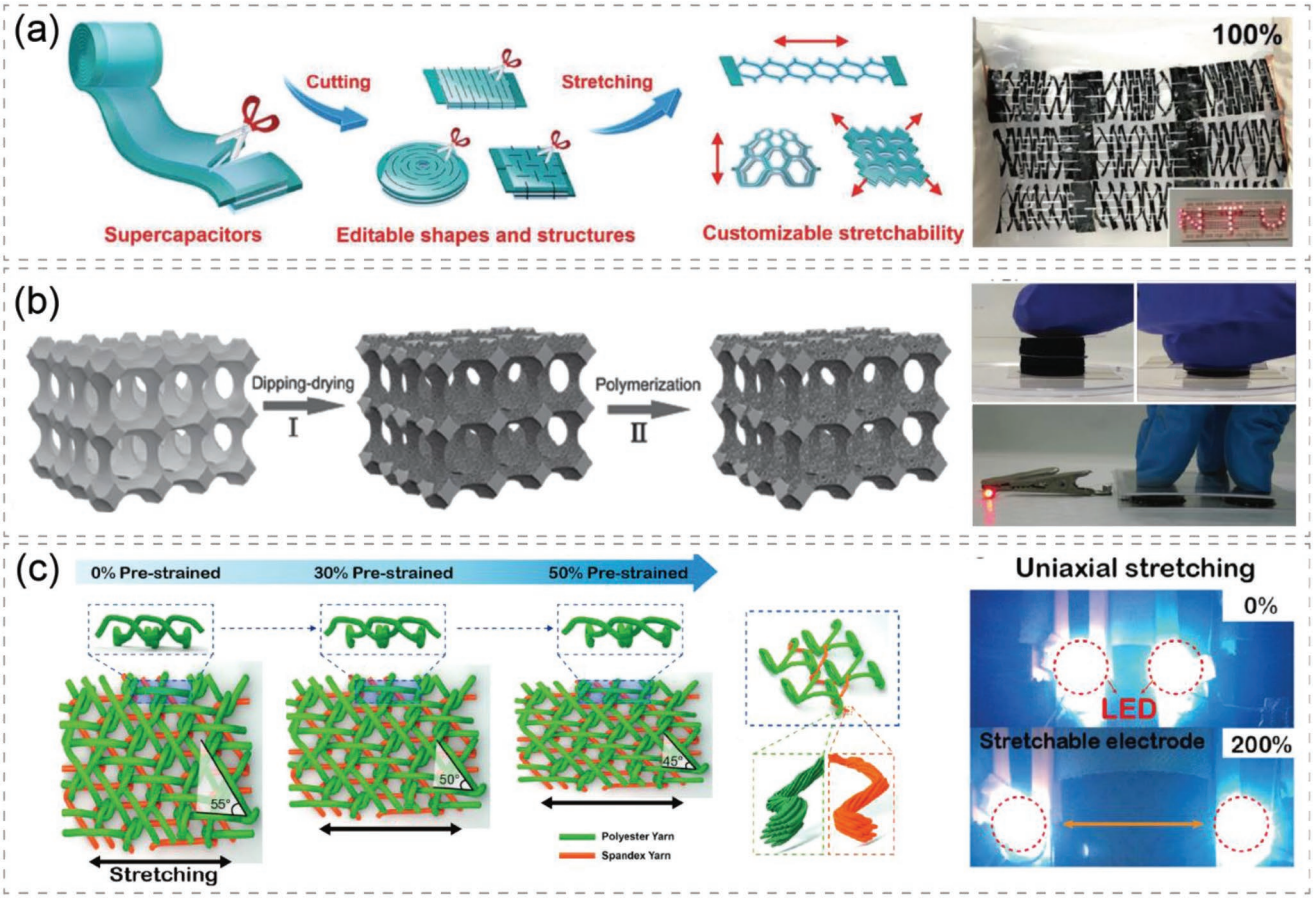

Figure 7. Schematic illustrations for three typical 3D stretchable supercapacitors. a) Editable assembling process to form kirigami-inspired structures with desirable shapes, including honeycomb-like, pyramid pop-up, and living-hinge shape. The as-fabricated supercapacitor array powered LEDs at the strain of 100%. Reproduced with permission.[161] Copyright 2017, WILEY-VCH Verlag GmbH & Co. KGaA, Weinheim. b) Fabrication process of PANI–SWCNTs sponge composite electrodes and images of compressing and revocering process to light an LED. Reproduced with permission.[164] Copyright 2015, WILEY-VCH Verlag GmbH & Co. KGaA, Weinheim. c) Weaving method to design textile structures and the changes of the polyester yarns during prestrain treatment. The as-prepared supercapacitor consistently powered LEDs upon uniaxial stretching up to 200%. Reproduced with permission. [169] Copyright 2015, American Chemical Society.

Sponge structure is an intrinsically compressible porous substrate with high internal specific surface area, representing a promising 3D scaffold for compressive supercapacitors.[55] Compression is the reverse of tensile stretching with negative strains. Thus, we consider compressible supercapacitor as a special type of stretchable supercapacitor. In a recent work, a compressible all-solid-state supercapacitor based on PANI–SWCNTs sponge electrodes with high compression tolerance was demonstrated,[164] as shown in Figure 7b. The electrical performance of as-prepared supercapacitors was almost unchanged when compressed under −60% strain. In another report,[165] a facile, green, and template-free approach was used to develop 3D sponge-like carbonaceous hydrogels and aerogels using crude biomass watermelon as the carbon source. By incorporating Fe_3O_4 nanoparticles into the carbonaceous gel networks and transforming them into magnetite carbon aerogels, the device exhibited a high capacitance of 333.1 F g^{-1} at a current density of 1 A g^{-1} and sustained large compressive strain of over −50% with complete recovery.

Recently, supercapacitors with a 3D textile configuration have drawn significant attention, owing to their high porosity and stretchability.[166] The conductive textiles made of SWCNTs electrodes showed good stretchability and high areal capacitance of up to 0.48 F cm^{-2} due to the strong adhesion between coating electrodes and textiles.[167] To further improve the areal capacitance, porous MnO_2 particles were doped into the textiles and an increase of 24-folds in capacitance was achieved. More importantly, the outstanding stretchability of the yarn textile mainly relied on the weaving strategy.[168] A pioneering work showed a tricot wavy structure alternately interwoven with inelastic and elastic hybrid yarns, constituting a repeating zigzag pattern,[169] as illustrated in Figure 7c. It provided excellent stretchability (up to 200%) and mechanical stability under dynamic strain operation. By increasing the inter-yarn contact, the resultant stretchable supercapacitor coated with MWCNTs achieved a sevenfold conductivity enhancement, reaching 33 000 S cm^{-1} even at 130% strain deformation.

Fabrication Methods for 3D Design: The kirigami-based structures are carefully designed to optimize omni-directional stretchability. Typically, the desirable architecture can be rationally designed into several deformable segments based on planar supercapacitors, enabling various types of electrical connections residing in one patch. In an important breakthrough that was reported, a simple and effective approach of graphitic conversion and laser cutting was used to design kirigami-inspired 3D stretchable structures.[160] The as-fabricated compliant structure could easily sustain more than 282.5% elongation with very small strain (<3%) in active electrodes. Besides cutting method, other strategies like template deposition can be used to construct kirigami 3D architectures. A pyramid-shaped CNT film was synthesized by depositing the catalyst on patterned template and CVD method. The 3D CNT film-based supercapacitor showed less than 7% capacitance change after stretching for 3000 cycles.[159]

3D sponge structures, commonly using CNT and graphene as electrodes, have been extensively reported, owing to their interconnected structure and high surface area. Several recent reviews have summarized the fabrication methods for 3D sponges of carbon materials.[17,170,171] Two main approaches are self-assembly and template method.[172–174] In self-assembly technique, CNT or graphene hydrogel is freeze-dried into CNT or graphene aerogel with sponge-like structure. For example, a sponge supercapacitor was developed with reversible compressibility, high elasticity, and durability by exploiting the PVA-assisted self-assembly followed by the cross-linking of rGO.[175] The resultant rGO aerogels were highly porous and lightweight, leading to an increase of >140% and >1400% in the gravimetric and volumetric capacitances, respectively, under -90% compression, compared to conventional rGO aerogels. In template method, the precursor fills the voids of the template, and then the templates are removed to obtain porous architecture after the solidification of precursors. For example, a 3D macroporous graphene structure was fabricated by utilizing self-assembled polystyrene (PS) colloidal particles as sacrificial templates.[176] The assembled asymmetric supercapacitor showed remarkable performance with 25 kW kg^{-1} power density and excellent cycle life.

The 3D stretchable textiles can be prepared by weaving and knitting with stretchable fiber electrodes or depositing electrodes on natural stretchable textiles. A brief overview of integrating these strategies into 3D textile supercapacitors is shown in Figure 7c. Researchers interwove polyester and spandex yarns alternately into zigzag pattern.[169] Although single polyester yarn was nonstretchable, the integrated textile was highly stretchable, tolerating strains up to 200%. Techniques such as adhesive bonding, ultrasonic welding, and laser welding are also used to fabricate textile supercapacitor, which may eliminate bulky stitched seams and enhance the stretchability of the biodevices.[177] However, owing to the strict requirements for the knitted yarns, it remains challenging for large-scale production of textile supercapacitors.

In summary, by combining novel materials with suitable design strategies, stretchable supercapacitors can be designed and tailored for specific applications. From the aspect of materials, a key concept is to replace the traditional rigid, bulky metal materials with intrinsically stretchable materials, ensuring consistent electrical performances at large strain levels. More importantly, the interface of the electrode materials needs special attention, since the delamination or cracks under large deformations may affect the performances. Depending on their architectures, 1D fiber supercapacitors are commonly weaved into textiles that can be used for wearable smart bioelectronics, 2D planar supercapacitors are utilized as patches for skin-mounted or tissue-mounted applications, and 3D supercapacitors of kirigami-inspired and porous structures are also widely used for wearable applications.

3. Health Monitoring Bioelectronics Powered by Stretchable Supercapacitor

Recent advances in materials, device configurations, and fabrication methods render the stretchable supercapacitors an energy storage unit with great potential in health monitoring bioelectronics. In this section, we provide an overview of emerging bioelectronics that were powered by stretchable supercapacitors and highlight key embodiments for integrating power source in health monitoring platforms with an emphasis on biocompatibility. We sort these applications into four categories, namely nontouching wearables, skin-touching wearables,

skin-conforming wearables, and implantables, with ascending intimacy with the body and thus increasing demand on biocompatibility. Bioelectronics woven on the clothes or shoes are categorized as nontouching wearables: these devices normally indirectly contact with the body, thus requiring relatively low biocompatibility. Bioelectronics attached to the human body are categorized as skin-attaching electronics, and those adhered to the skin with conformal contact are categorized as skin-conforming electronics, which are also known as electronic-skins and require relatively high level of biocompatibility to ensure irritation-free touching and avoid adverse reactions. In addition, devices implanted into the body for real-time physiological condition monitoring are categorized as implantables, which generally require sufficient biocompatibility to eliminate immune responses and even biodegradability on certain occasions. Representative works and corresponding metrics are summarized in **Table 1**.

3.1. Wearable Bioelectronics

Wearable bioelectronics powered by stretchable supercapacitors are expected to be worn on the human skin or integrated into clothes, shoes, and other accessories. Based on biocompatibility requirements, wearable devices can be classified into three types: nontouching, skin-touching, and skin-conforming devices.

3.1.1. Nontouching Wearables

Nontouching wearables can be designed on clothes by different methods, such as weaving stretchable fiber supercapacitors with textiles, directly printing electrode/electrolyte on fabrics, and permanently bonding onto clothes. Aside from being attached on clothes, nontouchable wearables can also be integrated onto gloves, wrist bands, or shoes, with suitable configuration designs like fiber or kirigami-based structure, as described below.

The most common nontouching wearables are stretchable fiber supercapacitors integrated with smart textile fabrics onto cloths.[178,179] For example, stretchable fiber supercapacitors were fabricated using twisted steel yarns coated with Ni—Co—S and rGO as positive and negative electrodes.[180] The yarns were then incorporated into elastic PDMS tubes to achieve a stretchability of 100%. After that, the stretchable fiber supercapacitors were arranged in arrays and integrated on clothes to power parallel LEDs, as shown in **Figure 8**a. They exhibited a high specific capacitance of 127.2 mF cm^{-2} under an operating voltage window of 1.7 V. To achieve a highly stretchable supercapacitor, intrinsically stretchable fiber electrode consisted of PPy/CNTs/UY with PVA/H_3PO_4 electrolyte were introduced.[181] The as-fabricated stretchable fiber supercapacitor exhibited a high areal capacitance of 69 mF cm^{-2} and a high stretchability of 130%. By integrating them into knitted fabrics, the wearable device could light an LED even under large stretches.

Besides weaving fiber supercapacitors on cloths, the electrodes/electrolytes of stretchable supercapacitors can be directly printed on fabrics for wearing comfort. Stretchable supercapacitors knitted and screen-printed on natural textiles as wearable electronics were reported, as shown in Figure 8b.[34] The scalable fabrication methods offered high areal mass loading while retaining the high intrinsic capacitance of active carbon electrodes. The wearable textiles had little loss in capacitance after being stretched to 50% and released. Inspired by stencil-printing strategy, printed AC/MWCNT/[EMIM][TFSI] electrodes and ionic-based gel electrolytes were adopted to form a wearable supercapacitors.[182] To ensure seamless unitization and design versatility of the printed supercapacitors, stainless steel threads were sewn on the T-shirt in advance as current collector before they were sealed with a water-proof packaging film. Notably, the printed stretchable supercapacitors on T-shirts could continuously supply power during wringing, ironing, laundering, and folding, indicating their great application potentials.

Nontouching supercapacitors can be bonded permanently to clothes for more stable performance. For example, a stretchable supercapacitor was fabricated and then firmly attached onto clothes to serve as power supply.[183] The stretchable supercapacitor utilized soluble PPy coated on carbon black as electrode, H_3PO_4/PVA as electrolyte, and elastic silicone rubber as packaging material. The supercapacitor attached onto clothes could harvest energy from movements by different parts of body, such as shoulder, wrist, and arm, as shown in Figure 8c. Such a fully enclosed structure was washable, water-proof, and stretchable (up to 100%). In another study, a shape-tailorable supercapacitor, which was fully functioning in severe conditions, such as being cut, punctured, or blasted, was proposed.[184] By integrating it with cloth, the device served as a reliable power supply and illuminated an LED even when both of the device and the cloth were partially damaged.

Apart from being worn on clothes, nontouching wearables can also be integrated into gloves, wrist bands, or shoes.[107,185] As illustrated in Figure 8d, a highly stretchable fiber supercapacitor with double-helical twisting structure was woven into a glove, showing little change in capacitance at finger movements.[186] The capacitance remained at 16.8 mF cm^{-2} while the supercapacitors were stretched up to 360%, and 85% of capacitance was sustained after 2000 stretching/releasing cycles under 200% strains. Similarly, a biaxially stretchable supercapacitor based on buckled hybrid fiber arrays has been attached to gloves.[187] For the integration on other wearables, a stretchable microsupercapacitor mounted on wrist strap has also been reported,[188] as shown in Figure 8e. The adopted honeycomb structure helped accommodate large deformations without producing excessive strain in the supercapacitors and interconnects. Such supercapacitor arrays showed excellent electrochemical performance and good mechanical stability under 275% stretching, bending, and twisting. In another study, a lightweight, stretchable, and tailorable supercapacitor based on activated carbon fiber veil was incorporated in shoes,[189] as shown in Figure 8f. The compressible supercapacitor located below a shoe insole could light up a red LED when being pressed by the weight of human body. The veil-based supercapacitor also exhibited good mechanical reliability against folding and cutting, owing to its kirigami structure. These reported works provided new possibilities in broadening the design options for health monitoring and improving the durability and comfort of wearing.

Table 1. Summary of wearable and implantable biodevices.

Application	Position	Materials (electrode @ electrolyte)	Configurations	Stretchability	Capacitance	Energy density	Retention	Refs.
Nontouching wearable	Clothes	Ni–Co–S/rGO @ PVA/LiOH	Wavy fiber	100%	127.2 mF cm^{-2} @ 1.7 V	10.19 mWh cm^{-3}	91% after 1000 cycles	[180]
	Clothes	PPy–CNTs–UY @ PVA/H_3PO_4	Textile	130%	69 mF cm^{-2} @ 5 mV s^{-1}	6.13 uWh cm^{-2}	85% after 1000 cycles	[181]
	Clothes	Woven CF @ SiWA	Textile	50%	0.51 F cm^{-2} @ 10 mV s^{-1}	–	80%	[34]
	Clothes	PPy–CB @ PVA/H_3PO_4	Sandwich	100%	2.4 mF @ 10 mHz	–	92% after 10 000 cycles	[183]
	Clothes	Ni–NiCoP/Ni–NiCoP–SWCNT @ PAM/KOH	Textile	100%	877.6 mF cm^{-2} @ 5 mV s^{-1}	40 mW cm^{-2}	100% after 1000 cycles	[246]
	Glove	AuNWs/AuFilm/PANI @ PVA/ H_3PO_4	Wavy fiber	360%	16.8 mF cm^{-2} @ 0.14 mA cm^{-2}	–	85% after 2000 cycles	[186]
	Glove	SWCNT/PEDOT @ PVA/ H_3PO_4	Bulked fiber	100%	53 F g^{-1} @ 1 A g^{-1}	6 Wh kg^{-1}	90.1% after 5000 cycles	[187]
	Glove	CNT @ PVA/LiCl	Bulked fiber	200%	11.88 mF cm^{-2} @ 10 mA s^{-1}	5.5 uWh cm^{-3}	94.8% after 1000 cycles	[107]
	Glove	CFT-PANI/FCFT @ PVA/ H_3PO_4	Wavy fiber	100%	4.8 F cm^{-3} @ 1.6 V	2 mWh cm^{-3}	81% after 10 000 cycles	[185]
	Wrist band	SWCNTs @ PVA/H_3PO_4	Interdigitated arrays	275%	0.15 F cm^{-3} @ 0.05 V s^{-1}	0.18 mWh cm^{-3}	90% after 10 000 cycles	[188]
Skin-touching wearable	Watch-band	CNF-PEDOT:PSS-CF @ PVA/H_3PO_4	Fiber arrays	100%	–	85 mW m^{-2}	70% after 6000 cycles	[236]
	Watch strap	PANI–CNT @ PVA/H_3PO_4	Kirigami	140%	340.2 mF cm^{-2}@2 mA cm^{-2}	0.701 mWh cm^{-3}	98.3% after 3000 cycles	[163]
	Skin	CNTs–RuO_2 @ PVA/H_3PO_4	Wavy planar	30%	7 mF cm^{-2} @ 0.5 mA cm^{-2}	–	95% after 2000 cycles	[237]
	Arm/knee	MWCNT/Mn_3O_4@PMMA/PC/$LiClO_4$	Interdigitated arrays	50%	8.9 F cm^{-3} @1.5 A cm^{-3}	1.8 mWh cm^{-3}	90% after 4500 cycles	[196]
	Hand	MWCNTs @ PEGDA/[EMIM][TFSI]	Interdigitated arrays	100%	0.51 mF cm^{-2} @ 0.006 mA cm^{-2}	0.34 μWh cm^{-2}	88% after 2000 cycles	[193]
	Hand	Graphite @ PVA/H_3PO_4	Kirigami	100%	1 mF cm^{-2} @ 10 mV s^{-1}	–	95% after 5000 cycles	[230]
	Forearm	MXene @ PVA/H_3PO_4	Kirigami	20%	23 mF cm^{-2} @ 0.1 mA cm^{-2}	2.8 mWh cm^{-3}	76% after 10 000 cycles	[235]
	Wrist	PPy–CNTs @ PVA/LiCl/MPII	Serpentine arrays	30%	5.17 mF cm^{-2} @ 100 μA cm^{-2}	0.44 μWh cm^{-2}	80% after 5000 cycles	[266]
	Wrist	WO_3-PEDOT:PSS @ PAAm-hydrogel	Sandwich	40%	471 F g^{-1}@1 V s^{-1}	52.6 Wh kg^{-1}	92.9%/50 000 cycles	[192]
	Wrist/neck	MWNT @ PEGDA/[EMIM][TFSI]	Interdigitated arrays	50%	4.7 F cm^{-3} @ 0.23 A cm^{-3}	1.5 mWh cm^{-3}	99% after 20 000 cycles	[256]
	Elbow	GO/GO–MnO_2 @ PVA/H_3PO_4	Interdigitated	150%	40.2 mF cm^{-2} @ 0.1 mA cm^{-2}	–	85.8% after 2000 cycles	[195]
Skin-conforming wearable	Finger joint	LIG-N-PEDOT @ PAAK/KOH	Interdigitated	400%	790 μF cm^{-2} @ 50 μA cm^{-2}	–	90% after 1000 cycles	[194]
	Finger joint	MWCNTs/Mn–Mo @ ADN/SN/LiTFSI/PMMA	Interdigitated	50%	7.5 mF cm^{-2} @ 0.3 mA cm^{-2}	4.2 μWh cm^{-2}	90% after 1000 cycles	[198]
	Epiderma	SWCNT/PEDOT @ PVA/H_3PO_4	Ultrathin planar	20%	56 F g^{-1} @ 1 A g^{-1}	6 Wh kg^{-1}	95% after 10 000 cycles	[197]
	Epiderma	EG/PH1000 @ PVA/H_2SO_4	Interdigitated	–	5.4 mF cm^{-2} @ 1 mV s^{-1}	–	90% after 5000 cycles	[199]
	Epiderma	v-AuNWs/PANI @ PVA/H_3PO_4	Ultrathin planar	–	11.76 mF cm^{-2} @ 10 mV s^{-1}	0.71 μWh cm^{-2}	93.6% after 2000 cycles	[200]
Implantable	Physiological fluids	CNT @ biological fluids	Fiber	–	10.4 F cm^{-3} @ 0.5 A cm^{-3}	–	98.3% after 10 000 cycles	[74]
	Subcutaneous of rat	MnO_2–MWCNT/AC @ body fluids	Fiber	–	–	–	99% after 1000 cycles	[75]
	Abdominal muscle of mouse	PEDOT:PSS/ ferritin/MWCNT @ PBS	Fiber	–	32.9 F cm^{-2} @ 10 mV s^{-1}	0.82 μWh cm^{-2}	90% after 8 d	[219]
	Mouse tissue	PANI-carbon @ PVA/H_3PO_4	Fiber	–	4 mF mm^{-2}	450 μJ mm^{-2}	–	[220]

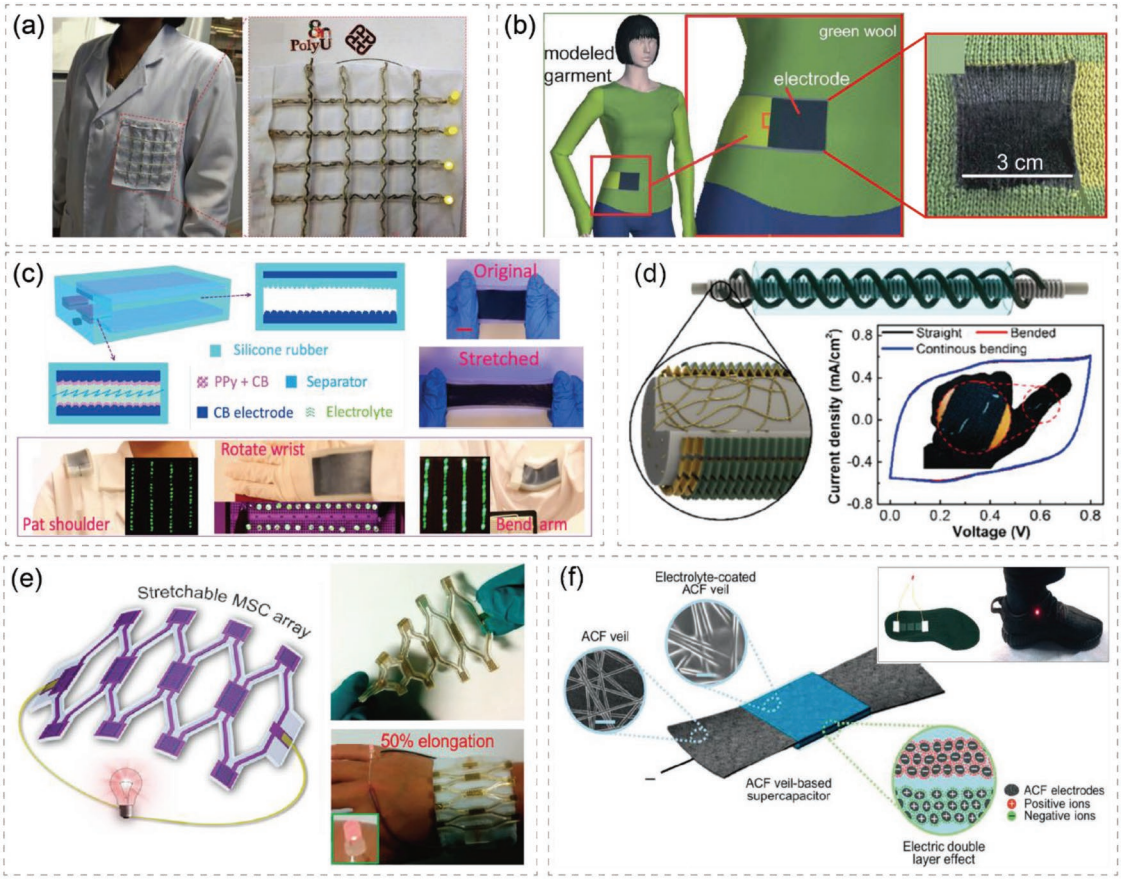

Figure 8. Representative applications of stretchable supercapacitors in non-touching wearables. a) Schemetic illustration of woven fiber-based supercapacitors integrated in clothes. Reproduced with permission.[180] Copyright 2018, WILEY-VCH Verlag GmbH & Co. KGaA, Weinheim. b) Stretchable supercapacitors printed on textiles and embedded as part of garments. Reproduced with permission.[34] Copyright 2013, The Royal Society of Chemistry. c) Bonding of the encapsulated stretchable supercapacitor onto clothes. Reproduced with permission.[183] Copyright 2016, American Chemical Society. d) Weaving of twisting fiber-based stretchable supercapacitors on gloves. Reproduced with permission.[186] Copyright 2018, American Chemical Society. e) Stretchable supercapacitors integrated on wrist strap which powered an LED under 50% elongation. Reproduced with permission.[188] Copyright 2016, American Chemical Society. f) Planar veil-based supercapacitors attached under a shoe insole which powered a red LED. Reproduced with permission.[189] Copyright 2018, WILEY-VCH Verlag GmbH & Co. KGaA, Weinheim.

3.1.2. Skin-Touching Wearables

Skin-touching wearables are directly attached on skins with higher biocompatibility requirement than nontouching wearables. These wearable devices, like watch bands, are typically encapsulated and mounted on the skin of bodily parts.[190,191] For instance, a stretchable supercapacitor based on CNT film electrode was developed to power a watch band, as shown in **Figure 9**a.[163] The typical cellular pattern endowed the strap with good stretchability of 140%, making it fit for people with different wrist sizes. After being charged to 4 V, supercapacitors in serial or parallel could successfully power a commercial electronic watch. Recently, a multifunctional wearable electrochromic device powered by all-transparent stretchable supercapacitor was developed (Figure 9b).[192] Attributed to the dual coloration and pseudocapacitive characteristics of PEDOT:PSS/WO_3 electrodes, the electrochromic wearable patch device enabled stable electrochemical properties even under repeated stretching-bending cycles. In addition, the incorporation of PAAm electrolytes not only enhanced the stretchability and electrochemical performance, but also solved the leakage problems during mechanical deformations, making the stretchable supercapacitor a promising multifunctional power supply.

Soft and skin-compatible substrates are often used to attach the stretchable supercapacitor with the human skin.[193,194] A plaster-like graphite-based microsupercapacitor was attached to skin by a medical tape with great skin adhesion (Figure 9c).[195] The medical adhesive tape is easy to wear and peel on skins, and thus the skin-mounted supercapacitors are convenient to be directly mounted on different parts of skin at various stretching or bending states. Alternatively, silicone-based substrates are sometimes used to encapsulate wearable devices and separated it from skin, ensuring biocompatibility of the device. For example, a supercapacitor encapsulated in stretchable Ecoflex substrate could be directly attached to skin using silicone adhesives, as shown in Figure 9d. The stretchable supercapacitor incorporated a layer-by-layer assembled MWCNT/Mn_3O_4 thin film as electrodes and PMMA/PC/$LiClO_4$ as electrolytes.[196] The device exhibited high mechanical stability under

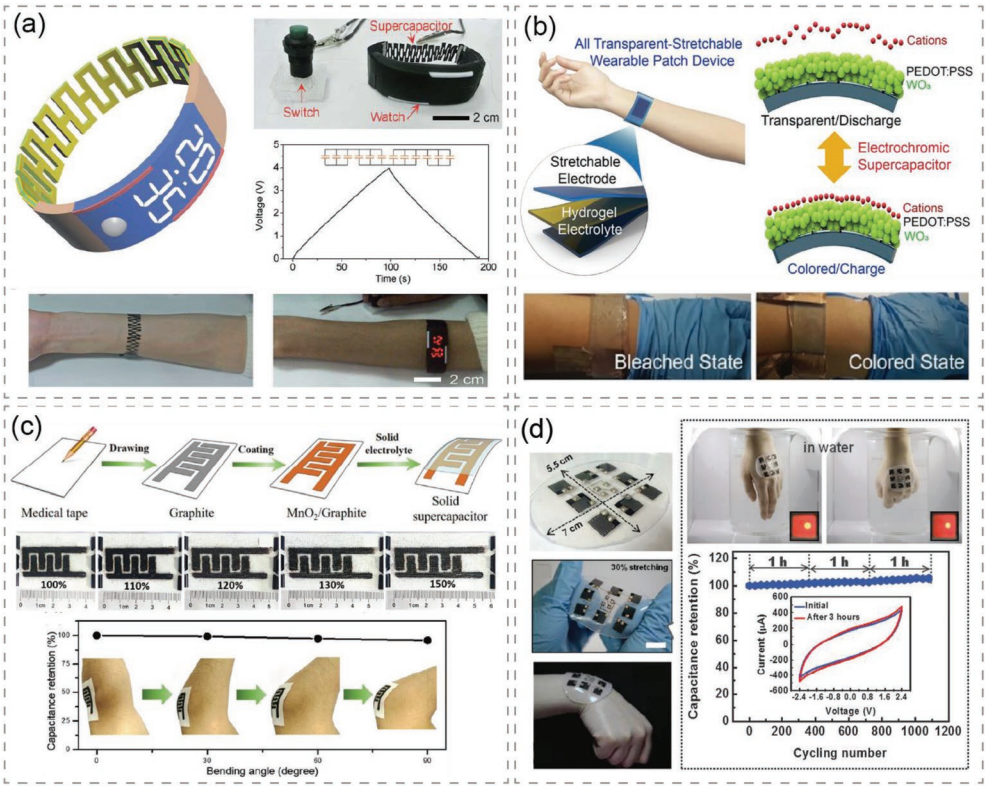

Figure 9. Representative applications of stretchable supercapacitors in skin-touching wearables. a) Stretchable supercapacitors integrated on a watchband with cellular structure to power an electronic watch. Reproduced with permission.[163] Copyright 2016, The Royal Society of Chemistry. b) Schematic illustration of an all-transparent stretchable electrochromic supercapacitor attached to the wrist as a wearable patch device. Reproduced with permission.[192] Copyright 2019, American Chemistry Society. c) Fabrication process of thin-film stretchable supercapacitors and the as-fabricated device under various stretching states. The capacitance retention of the skin-mountable device showed little change under different bending states with elbow bending from 0° to 90°. Reproduced with permission.[195] Copyright 2018, WILEY-VCH Verlag GmbH & Co. KGaA, Weinheim. d) Encapsulated stretchable supercapacitors attached to the wrist and immersed in water. Reproduced with permission.[196] Copyright 2015, The Royal Society of Chemistry.

uniaxial and biaxial stretching up to 50% and possessed stable electrochemical performance under repeated cycles of attachment-detachment on skin, even exposure to water, implying the robustness of such devices.

3.1.3. Skin-Conforming Wearables

Skin-conforming wearables, also referred to epidermal, skin-like, or skin-conformal devices, are thin (<1 mm) and ultralight devices that can adhere noninvasively and intimately onto epidermis with high requirements of biocompatibility and comfort. These devices are also required to have good stretchability and flexibility to allow for adaptability and compliance, given that these devices are constantly subjected to stretching, twisting, compression, and bending. In this section, stretchable supercapacitors with small strains are summarized for skin-confirming wearables.

Epidermal supercapacitor with overall device thickness of only 1 μm was developed with superior electrochemical performance based on a SWCNT/PEDOT hybrid film,[197] as shown in **Figure 10**a. It could be adhered to skin with PVA or waterproof eyelash adhesive with good biocompatibility and stretchability. When mounted on fingers, an LED could be illuminated at various deformations. Intriguingly, the ultrashort response time of 11.5 ms manifested that such an epidermal supercapacitor was possible for high-power units. Other skin-like, dynamically stretchable supercapacitor with a thickness of 270 μm was developed, as shown in Figure 10b.[198] The supercapacitor consisted of buckled MWCNT/Mn–Mo electrodes and organic gel electrolytes. By depositing materials on a prestrained porous PDMS/Ecoflex substrate, the as-designed supercapacitor exhibited biaxially stretchability up to 50% strain and sustained 90% capacitance after 1000 stretching/releasing cycles. When attached to index finger, the device possessed excellent performance under dynamic stretching in real time and worked reliably during repetitive bending or spreading motions. Similarly, a skin-conformal supercapacitors fabricated by a novel direct printing method was demonstrated,[199] as shown in Figure 10c. The printable graphene and hybrid inks could be fabricated on an ultrathin PET substrate (<5 μm), offering stable performance. When the ultrathin device was attached to fingers or other body parts, it demonstrated stretchability, flexibility, and biocompatibility.

Multifunctionality, such as electrochromic property and degradability, can be incorporated into the next generation wearable biodevices. For supercapacitor with electrochromic property, the colors of electrodes vary under different voltages,

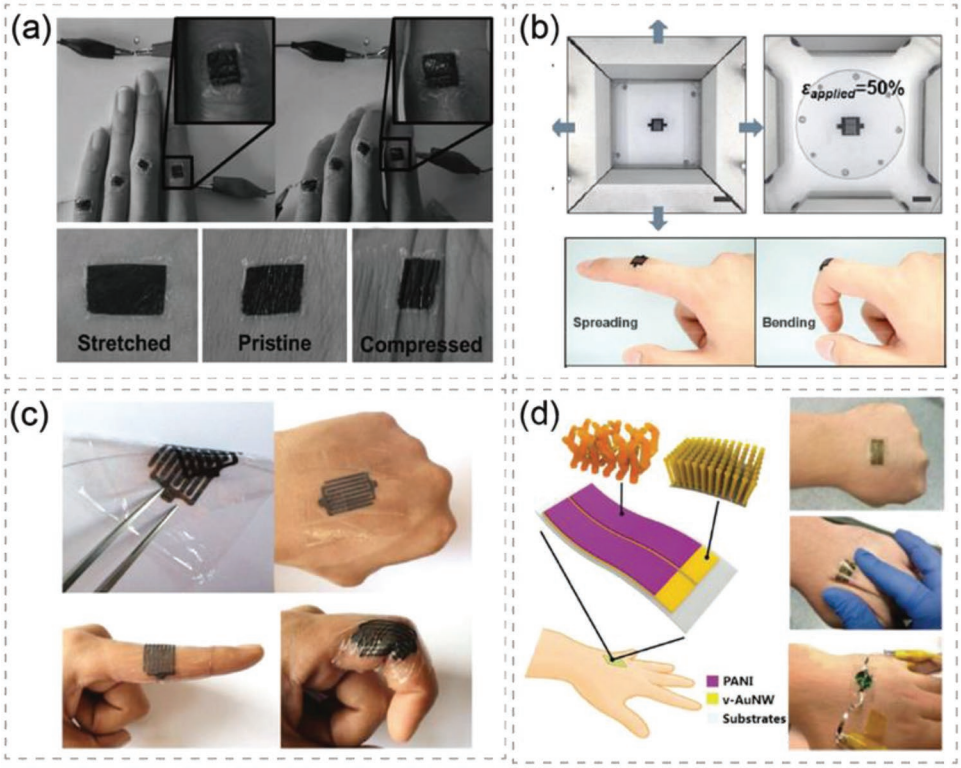

Figure 10. Representative applications of stretchable supercapacitors in skin-conforming wearables. a) Images of epidermal supercapacitors powering a LED when mounted in series on fingers with fingers being straight or bent and images of supercapacitor attached on wrist when the skin was stretched, pristine, and compressed. Reproduced with permission.[197] Copyright 2016, WILEY-VCH Verlag GmbH & Co. KGaA, Weinheim. b) Skin-conforming stretchable supercapacitors attached to an index finger with stretching deformations up to 50%. Reproduced with permission.[198] Copyright 2019, American Chemical Society. c) Ultrathin supercapacitors attached on hands and conforming to bent fingers. Reproduced with permission.[199] Copyright 2016, WILEY-VCH Verlag GmbH & Co. KGaA, Weinheim. d) Schematic illustration of skin-conforming electrochromic supercapacitor attached on skins. Reproduced with permission.[200] Copyright 2019, WILEY-VCH Verlag GmbH & Co. KGaA, Weinheim.

and thus the energy level of supercapacitors can be monitored easily by naked eyes. For instance, an ultrathin supercapacitor using gold nanowires and PANI electrodes was fabricated, in which PANI changed its colors between green and blue reversibly during charge/discharge cycles,[200] as illustrated in Figure 10d. The as-assembled device was patterned into skin-conforming patches on a hand through adhesive tape. It offered superior skin-conformability under both extremely static bending/stretching and arbitrary deformations. Other skin-mounted devices can be integrated with various sensor systems to monitor physiological parameters. For the sake of environment protection, disposable wearable devices for sustainable energy storage should be non-toxic and even degradable. Recently, a biodegradable, stretchable supercapacitor (160 μm) was reported, in which water-soluble transition-metal electrodes, hydrogel electrolyte, and a biodegradable substrate were all encapsulated in polyanhydride.[201] The devices could be easily attached to fingernails firmly, offering mechanical stability under folding, bending, and rolling deformations. It also showed stable performance when immersed in PBS solutions at physiological temperatures for a sufficiently long time. These results demonstrated their potential as power supply for wearable bioelectronics.

In summary, skin-conforming supercapacitors with high stretchability could be easily adhered onto epidermis and conformed to the tissue motion precisely, showing great potential in developing self-powered skin-like bioelectronics for human activity monitoring.

3.2. Implantable Bioelectronics

A major goal of bioelectronics is to realize real-time in vivo health monitoring and medical intervention with implanted functional devices, such as radio transmitters,[202] automated drug delivery systems,[70,203] sensors,[204,205] pacemakers,[206] stimulators for deep brain,[207] artificial visions,[70] and diagnostic/therapeutic devices.[208,209] Stretchable supercapacitors can potentially be used in implantable electronics as they can supply energy in a durable and continuous way. However, implantable supercapacitor works inside the human body and it represents a great challenge especially on biocompatibility. Therefore, seamless integration with biocompatible materials, long-term durability, and good user comfort in biological conditions are crucial. Traditional supercapacitors are fabricated from rigid materials that are ill-matched to soft tissue and materials are unstable and even toxic, which limits their practical applications. In this section, recent advancements in implantable applications with biocompatible electrodes/electrolytes and encapsulated supercapacitors are discussed.[210–217]

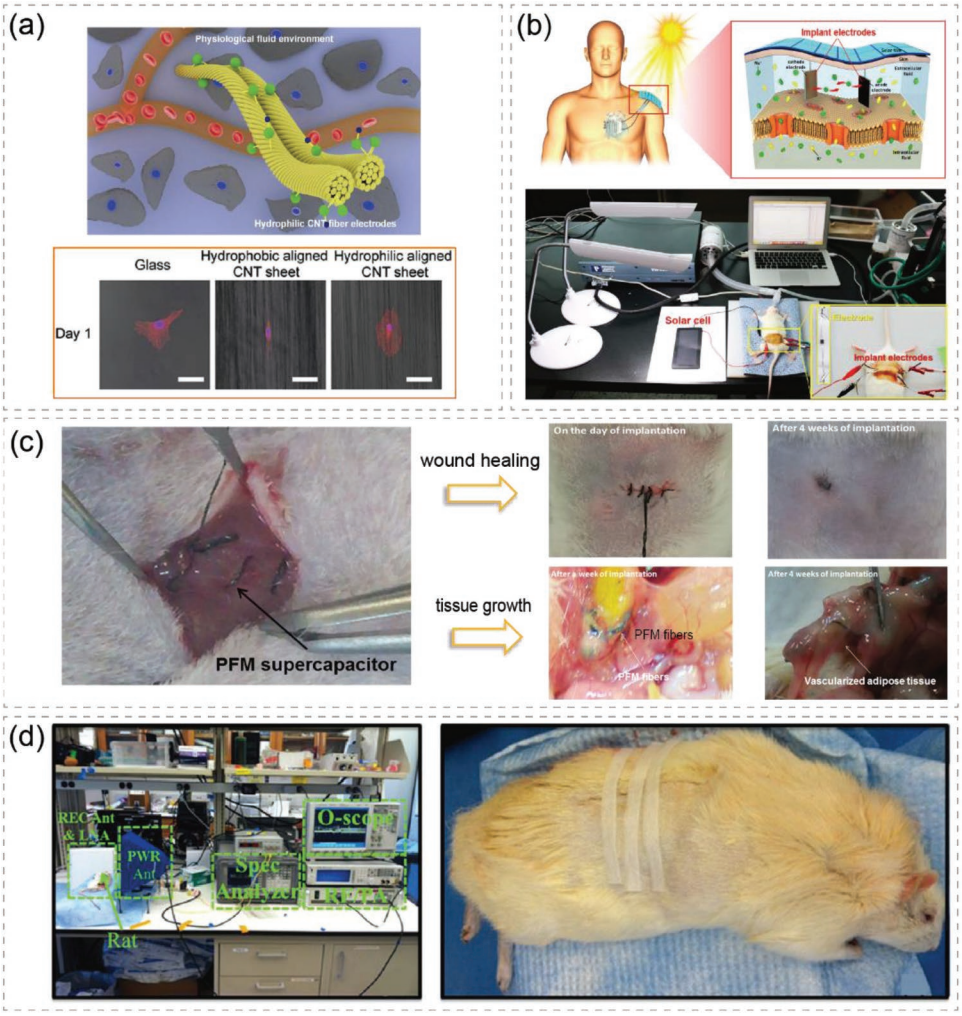

Figure 11. Representative applications of stretchable supercapacitors in implantables. a) Schematic of a biocompatible supercapacitor working in physiological fluids and the biocompatibility tests of differently aligned CNT sheets. Reproduced with permission.[74] Copyright 2017, Elsevier Ltd. b) Schematic of the components of the CNT/MWCNT device working in biological fluids and the as-fabricated device implanted into subcutaneous layer of a rat. Reproduced with permission.[75] Copyright 2017, Elsevier Ltd. c) Photograph of the PEDOT:PSS/ferritin nanoclusters coated MWCNT fibers implanted into the abdominal cavity of a mouse and optical images of implanted fiber supercapacitors on wound healing and vascularized adipose tissue surrounding. Reproduced with permission.[219] Copyright 2018, Elsevier Ltd. d) Photograph of the experimental setup and implanted mammal with the epoxy resin-packaged PANI-coated carbon cloth supercapacitor using PVA/H_3PO_4 gel electrolyte. Reproduced with permission.[220] Copyright 2018, Springer Nature.

Given the importance of biocompatibility in implantable devices, biological fluids are highly promising candidates, which can function as electrolytes. A novel biophilized reduced graphene oxide–protein supercapacitor with biofluid electrolytes was reported.[70] In this system, protein offered pseudocapacitive behavior with nanostructure that enhanced the ions transferring, showing good electrochemical performance with a capacitance of 534 F cm^{-3} in human urine and 372 F cm^{-3} in calf serum, respectively. Biocompatibility tests using mouse embryo fibroblasts and COS-7 cell lines showed no toxicity. Similar studies have utilized carbon nanotubes and graphene[218] as electrodes and generated nontoxic supercapacitors. For example, a biocompatible supercapacitor used hydrophilized CNT fibers as electrodes and phosphate buffered saline (PBS) solution, serum, and blood as direct electrolytes was reported (**Figure 11**a).[74] The supercapacitor achieved a capacitance of 10.4 F cm^{-3} and maintained with a retention of 98.3% after 10 000 cycles when working in physiological fluids. The adopted hydrophilic CNTs possessed better biocompatibility than hydrophobic CNTs, as proved by cytotoxicity tests on fibroblasts.

Body fluids have relative low operating voltage window, which limited the performance of biofluid-based supercapacitors. To address this problem, an asymmetric supercapacitor was developed, which widened the operation voltage when the supercapacitor was immersed in body fluids, as shown in Figure 11b.[75] In this device, MnO_2/MWCNTs was chosen as the positive electrode, and the negative electrode was made of phosphidated activated carbon. To assess the toxicity risks, in vitro cytotoxicity tests were performed using human-derived fibroblasts and African green monkey kidney COS-7 cells. Although MnO_2 was highly toxic to fibroblast cells, when

embedded in the MWCNTs, only 0.1 ppm of Mn^{2+} ions were produced, which was below the toxicity concentration levels in both in vitro and in vivo. The supercapacitor was then implanted into the subcutaneous layer of a Wistar rat and charged with a mini solar cell. It showed good performances and operated at a voltage window from 0.2 to 1.0 V at a current of 2 mA. The capacitance retention was stable at 99% with long-cycle life.

Furthermore, an implantable fiber-like supercapacitor was reported and implanted in mouse.[219] The electrodes were composed of MWCNT-coated PEDOT:PSS/ferritin nanoclusters with good mechanical strength and electrical conductivity. The device was then immersed in PBS solution and showed a capacitance of 32.9 mF cm^{-2} and an energy density of 0.82 μWh cm^{-2}. Subsequently, the supercapacitor was implanted into a BALB/c mouse and attached to abdominal muscle. No signs of infection or adverse effects were observed after implantation for four weeks, as a result, the sutured wound of the mouse was healed and the fibers were covered by vascularized adipose tissue, as illustrated in Figure 11c. Moreover, the capacitance retained 90% of its value after 8 d with high potential in blood vessel and wound. Another study reported an energy harvesting unit-integrated supercapacitor implanted inside a rat, showing a high operating energy storage density of 450 μJ mm^{-2}.[220] The electrode of supercapacitor was made of PANI-coated carbon cloth, and the electrolyte was PVA/H_3PO_4 gel encapsulated into Kapton tape. The whole system was packaged in epoxy resin and then placed subcutaneously on a rat. The device also incorporated a rectenna to harvest energy from incoming wireless signals, which was then transferred to the supercapacitor to power a transmitter for 8.5 s on the mouse tissue (Figure 11d). These pioneering works demonstrated the application potential of stretchable supercapacitors in implantable bioelectronics.

4. Integrated Bioelectronics with Stretchable Supercapacitors

Integrated bioelectronics usually include energy harvesting unit, energy management unit, and functional unit. The successful utilization of stretchable supercapacitors in health monitoring bioelectronics normally requires feasible integration of self-charging unit for energy harvesting and sensing unit for functional element into a single device. It is highly sought to couple supercapacitors with energy harvesting units, which collect energy from human body to charge supercapacitors and power biodevices, thus eliminating the need of frequent charging from external power sources. This is especially true for the case of implantable biodevices, where charging or battery replacement requires surgeries. Therefore, extensive efforts have been devoted to searching for suitable energy sources with reliable converting strategies and integrating them with bioelectronic systems for diagnostic and therapeutic purposes.[221–226] In this section, we first present the existing energy harvesting strategies that have been applied to charge stretchable supercapacitors in health monitoring devices. We then discuss different sensing mechanisms of different sensing targets and provide insights on stretchable supercapacitor specifications.

4.1. Energy Harvesting Units

Human body constantly conveys energy in several forms such as mechanical motion and body heat. Energy exists in the environment, in the form of solar energy and radio frequency, can also be continuously transferred and collected. To charge supercapacitors with these easily accessible energy sources, a few energy converting strategies have been adopted, based on effects such as triboelectric, piezoelectric, photovoltaic, thermoelectric, and electromagnetic induction. In the following sections, we summarize recent progresses of stretchable supercapacitors that integrated energy harvesting units as a self-powered device, with emphasis on the potentials for health monitoring bioelectronics.

4.1.1. Triboelectric

When two objects of different materials are in contact, due to their different tendency to lose or gain electrons, the two contacting surfaces will be oppositely charged in a process called triboelectric effect. Based on this effect, triboelectric nanogenerator (TENG) was developed and have found profound applications in the harvesting of motion energy.[227] To achieve efficient energy conversion, a wide array of materials has been utilized, including both organic (PTFE, PDMS, PMMA, CNTs, and graphene) and inorganic (ITO, Si, Al, Ti, and TiO_2) materials. To efficiently harvest motion in different forms and charge stretchable supercapacitors, four configuration modes have been adopted, including contact-separation, lateral-sliding, single-electrode, and freestanding triboelectric-layer mode,[228,229] as illustrated in **Figure 12**.

Contact-separation mode generates current when two surfaces separate after contact.[230] For instance, TENG cloth was combined with stretchable yarn supercapacitor to fabricate a self-charging textile, as shown in Figure 12a.[231] When the TENG cloth was in contact with the cotton cloth, triboelectric effect occurred. Once they were separated, the flowing of electrons between two separated Ni coatings yielded a current through the external circuit. Thus, the repeated processes of contacting and separating could lead to an alternating output voltage about 40 V at 5 Hz. The integrated self-charging supercapacitor system was stretchable, owing to the stretchability of both the TENG and yarn supercapacitors. Similarly, arch-shaped TENG was integrated with stretchable supercapacitor into a single device. It was placed in shoe insole and used to generate electricity from mechanical vibrations, which could charge supercapacitors to a voltage of 3 V in 117 min.[232]

Lateral-sliding mode generates current while two surfaces slide over each other. For example, a wearable device used TENG in lateral-sliding mode with PU/PI and PDMS/Al materials patterned on conductive carbon fabric, as shown in Figure 12b. When woven into cloths near the armpit, the two TENGs slid over each other closely to obtain electrical current, generating electricity output with a power density of 0.18 μW cm^{-2} at 1.5 Hz.[233] Recently, a bioinspired stretchable TENG with a strain up to 600% was developed as an energy-harvesting E-skin.[234] This TENG consisted of patterned interconnected cellular structures, and physiological saline was used as electrodes,

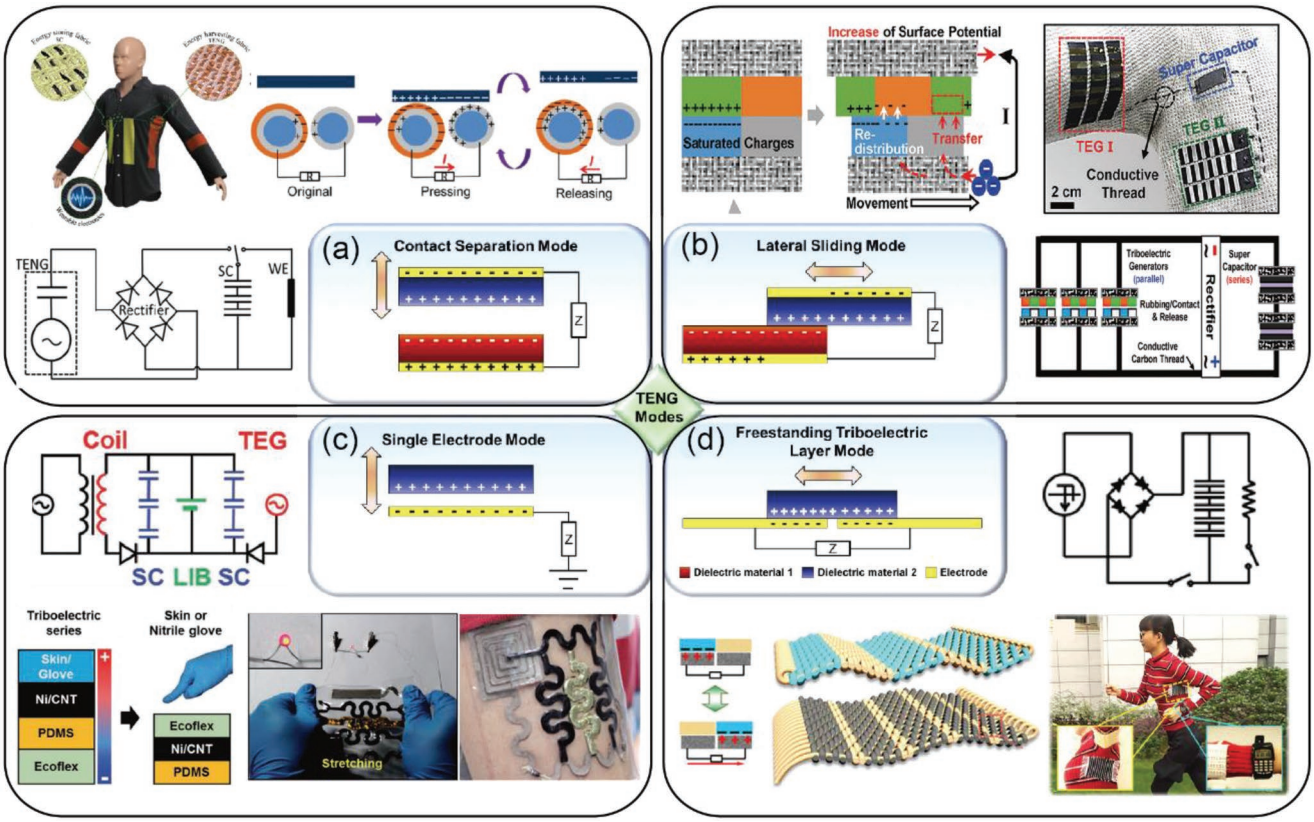

Figure 12. Schematics of working modes of triboelectric nanogenerators (TENGs) for stretchable supercapacitor charging and representative applications. Schematics of working modes reproduced with permission.[228] Copyright 2017, AIP Publishing. a) Contact seperation mode and the integration in fabrics to power wearable electronics. Reproduced with permission.[231] Copyright 2015, WILEY-VCH Verlag GmbH & Co. KGaA, Weinheim. b) Lateral silding mode and the integration in clothes with conductive thread connection. Reproduced with permission.[233] Copyright 2014, WILEY-VCH Verlag GmbH & Co. KGaA, Weinheim. c) Single electrode mode and the integration in a skin-conforming device. Reproduced with permission.[237] Copyright 2017, WILEY-VCH Verlag GmbH & Co. KGaA, Weinheim. d) Freestanding triboelectric layer mode and the integration in clothes to power a watch. Reproduced with permission.[238] Copyright 2018, Elsevier Ltd.

exhibiting an instantaneous power density of 2.65 mW m^{-2} at 2.3 Hz. The device was biocompatible and thus suitable for wearable and implantable applications.

Single-electrode mode adopts only one electrode and generates electric potential against the ground without the need of a spacer, thus facilitating the integration of TENG and supercapacitor in a sealed thin-film. For example, a compact self-powered system integrating TENG in single-electrode mode was reported, where MXene-based stretchable supercapacitor was attached onto skin as the ground electrode.[235] The reported device generated electricity continuously from regular human activities with little current leakage. Although this mode of TENG had great application potential, difficulty in fabrication process posed a challenge. A facile and scalable weaving method was employed to fabricate and integrate an hybrid fiber supercapacitor and TENG into textiles.[236] The integrated self-charging system had high stretchability of 100%, and it could power LEDs, a temperature–humidity meter, and a calculator with a maximum peak power density of 85 mW m^{-2}. Recently, a system that integrated stretchable wireless power transmission, TENG, LIB, and supercapacitor was successfully fabricated.[237] In this integrated system, the metallic coil charged the LIB and supercapacitor wirelessly, and the TENG accelerated the charging rate. The power generation of the integrated device was maintained even under stretch up to 30%, as shown in Figure 12c.

Freestanding triboelectric-layer mode consists of symmetric electrodes beneath a dielectric layer with equal size. It harvests energy from mechanical motion without an attached electrode. When the upper object approaches to or departs from the electrodes, it generates charge distribution through induction effect and make electrons flow between the two electrodes to balance the local potential distribution. From the perspective of physical contact, this mode does not induce materials abrasion or generate heat, which distinguishes itself from other modes. Traditional woven craft was used to fabricate a one-piece self-powered textile, which collected energy through running or walking and simultaneously powered a watch, as shown in Figure 12d.[238] The as-designed device had good performance at a working frequency of 2 Hz for 5 h.

4.1.2. Piezoelectric

Piezoelectric nanogenerator (PENG) offers an alternative approach to TENG for harvesting mechanical energy based on piezoelectric effect in health monitoring devices. In PENG, materials

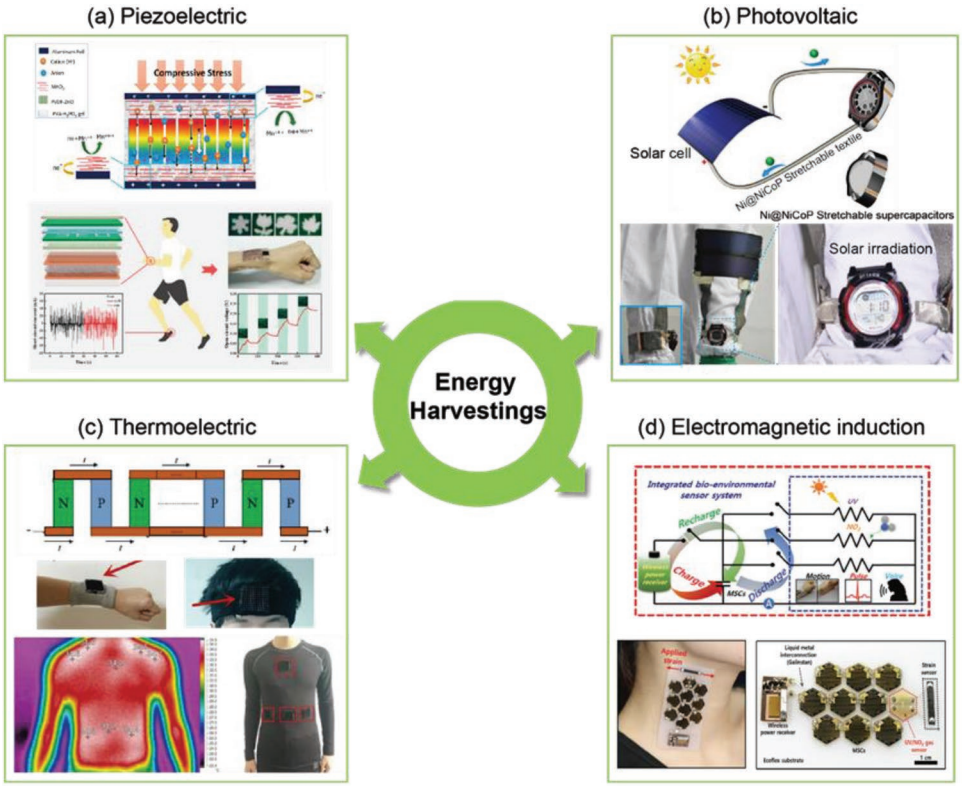

Figure 13. Other energy harvesting strategies and corresponding applications based on different energy conversion including piezoelectric effect, photovoltaic effect, thermoelectric effect, and electromegnatic induction, as indicated. a) The mechanisms of piezoelectric nanogenerators for the harvesting of energy from human movements. Reproduced with permission.[239] Copyright 2015, American Chemical Society. And a representative application. Reproduced with permission.[242] Copyright 2019, American Chemical Society. b) An application of photovoltaic effect to charge supercapacitors on a coat to power an electronic watch. Reproduced with permission.[246] Copyright 2019, Elsevier Ltd. c) The mechanism of thermoelectric generators connected in series and its application in harvesting energy from human skin. Reproduced with permission.[251] Copyright 2017, IEEE. d) The circuit and an application of harvesting the energy from radio frequency to charge stretchable supercapacitors and power a multisensor system. Reproduced with permission.[256] Copyright 2015, WILEY-VCH Verlag GmbH & Co. KGaA, Weinheim.

like PVDF, PVDF-TrFe, PZT, or ZnO[239] are used to generate electricity in response to a dynamic pressure signal.[240,241] For example, a self-powered device with wearable PENG and electrochromic supercapacitor was reported for the immediate visualization of energy level.[242] Using PVDF nanofibers as the piezoelectric material, kinetic energy from human body, including elbows, knees, and feet during walking and running, was collected to charge a supercapacitor, as shown in **Figure 13**a. After four self-charging and discharging cycles for 50 s, the voltage of supercapacitor increased to 0.231 V. In another work, Maitra et al. fabricated a PENG using natural biomaterials, namely fish swim bladder, to collect electricity from human body motions and charge supercapacitors to 281.3 mV in 80 s.[243]

4.1.3. Photovoltaic

Photovoltaic (PV) devices provide a way to generate electricity from light, most commonly sunlight.[244,245] However, the intensity of the sunlight varies greatly depending on weather, season, and location, leading to an unstable electricity output. Therefore, it is necessary to integrate PV devices with energy storage such as supercapacitor to provide consistent power supply. As an example, a stretchable Ni/NiCoP textile supercapacitor was combined with flexible solar cells to form a self-powered energy storage unit, which is then applied on a lab coat, as shown in Figure 13b.[246] The resultant unit could power an electronic watch continuously with or without the sunlight, showing prominent in long-term use. Photovoltaic devices can also be designed in fiber configuration with high stretchability. The electrodes in fiber-shaped photovoltaic device can be shared with a fiber-shaped supercapacitor, which can significantly reduce the weight of the integrated device. A smart textile with both fiber-shaped photovoltaic devices and supercapacitors was demonstrated, in which they were tailored in any desirable patterns without losing their potential output.[247] The supercapacitors could be charged by solar energy to 1.2 V in 17 s and discharged for 78 s at 0.1 mA current. However, the intermittent and unpredictable nature of solar energy is an inevitable challenge to achieve consistent power supply in bioelectronics. To compensate for this, a hybrid system which integrated TENG, PV, and supercapacitor was reported, in which multiple energies were simultaneously collected from both sunlight and body motions.[248] The hybrid device was robustly flexible with a high power conversion efficiency of 5.64%, showing great potential in designing sustainable bioelectronics.

4.1.4. Thermoelectric

The temperature of human body is about 37 °C and body heat provides a steady renewable energy source.[249] Thermoelectric generator (TEG) uses Soret effect to convert the temperature gradient between the skin and the ambient into several milliwatts electricity through a thermopile.[250] Although the power density is relatively low due to the small temperature gradient, this strategy yields a continuous and stable power supply. These advantages are especially beneficial for skin-mounted devices for long-term operation. For example, a wearable thermoelectric power generator was integrated with stretchable supercapacitor into cloths for low-power human diagnosis devices, as shown in Figure 13c.[251] The device used body heat to continuously charge the supercapacitor. The harvested thermal energy could vary significantly depending on factors such as skin temperatures, ambient temperatures, wind, human activity, and the connected modes of TEG module. Moreover, since the human body has high thermal resistance, heat dissipated from the skin is only about 3–5 mW cm^{-2} on average.[252] Thus, TEG is typically utilized in combination with supercapacitors and PV to enhance power density. For instance, a self-powered medical device that could collect energy from body heat and ambient light was introduced.[253] These devices could be attached on arm or head and showed a thermoelectric efficiency of 0.4%.

4.1.5. Electromagnetic Induction

Electromagnetic induction offers a means to harvest radio frequency (RF).[254] Though the energy density of RF is low, it can work in extreme environments where solar energy and other energy sources are not available. RF energy can be harvested from ambient electromagnetic waves generated by broadcasting and wireless communication devices.[255] Kim et al. reported a stretchable self-powered system with a wireless power receiver and a supercapacitor array to power multisensors.[256] The electricity generated from wireless power receiver could stably charge the connected supercapacitors, as shown in Figure 13d. When the system was directly attached on the neck, it showed a high efficiency of 66% with load resistance of 2.2 kΩ and input power of 0.4 W, indicating the potential of RF in powering sensors for health monitoring. In addition, wirelessly rechargeable supercapacitor is a good choice to monitor the implanted healthcare and therapeutic devices remotely.

4.2. Sensing Units

Toward practical health monitoring bioelectronics, precisely detecting and analyzing physiologically relevant signals are essential, which requires reliable sensors in the integrated bioelectronic systems. Information collected from these sensors can then be used for early diagnosis and therapeutic decision making.[257,258] Therefore, reliable integration of stretchable supercapacitors and sensors have been of great significance in many biomedical applications.[259,260] In this section, we summarize the integrated sensing units in health monitoring devices for the measurement of physical and chemical/biochemical parameters.

4.2.1. Sensing of Physical Parameters

Many physiological conditions are related to variations in the local strain, pressure, or temperature.[261–263] For example, pulse and heart rate can be deduced by measuring the pressure on the blood vessel, and body movements can be tracked by measuring the strain at joints.[264,265] Here, we present a brief overview of advances in measuring physical signals including strain/pressure and temperature, highlighting integrated stretchable supercapacitors as energy storage to power different sensors.

Motions lead to different strains/pressures exerted on the sensors, which can be reflected by the variation in the electrical properties of the sensors, such as conductivity and capacitance. For example, a strain sensor and a stretchable supercapacitor were combined to detect useful physiological signals, such as arterial pulse and heart-beat.[266] In this work, PV generator was incorporated to collect solar energy, which was then stored in supercapacitors to power the sensor. After attaching the entire device on the wrist, as shown in **Figure 14**a, the arterial pulse could be mapped. Similar studies have been introduced by attaching the integrated devices on the neck to detect carotid artery pulses or heart rate in real time, and on the muscles to detect movements of drinking, swallowing, breathing, and coughing.[267–270]

Piezoresistive sensor system incorporating a supercapacitor and a piezo-resistor could detect movements.[262] For instance, a CNT–PDMS sponge based system consisting a stretchable supercapacitor and a compressible piezoresistor with remarkable sensitivity was reported.[271] When attached on the neck, the sensor could detect different pressure signals of body movements, such as speech, walk, and respiration (Figure 14b). In another work, an all-in-one piezoresistive-sensing patch was fabricated to detect motions, including touching and wrist/arm-bending.[265] The patch could be used as a self-powered 3D touch screen with a high sensitivity of 0.51 kPa^{-1} in the detection range of 0–2 kPa. This device also possessed a good mechanical reliability after repeated use and showed good quality in terms of safety communication and user identification.

To measure temperature, an asymmetric fiber supercapacitor and a temperature sensor were united.[263] The integrated device detected the temperature in a wide range from 30 to 80 °C with a high sensitivity of 1.95% $°C^{-1}$. Moreover, a self-powered multisensory system that could detect pressure/strain and temperature simultaneously was also developed, as shown in Figure 14c.[272] The integrated system exhibited a sensitivity of 2.01 kPa^{-1} for pressure below 1 kPa, high durability over 10 000 cycles, high thermoelectric sensitivity of 49.8 μV K^{-1}, and a fast response time of 20 ms.

4.2.2. Sensing of Chemical/Biochemical Parameters

Chemical/biochemical sensors exploit the electrochemical activity of the chemical species to detect their presence and concentration. One of the straightforward and noninvasive way to detect concentrations of small molecules in the human body is via perspiration.[258] For instance, the concentration of glucose and Na^+ and K^+ ions could be detected by analyzing the chemical composition

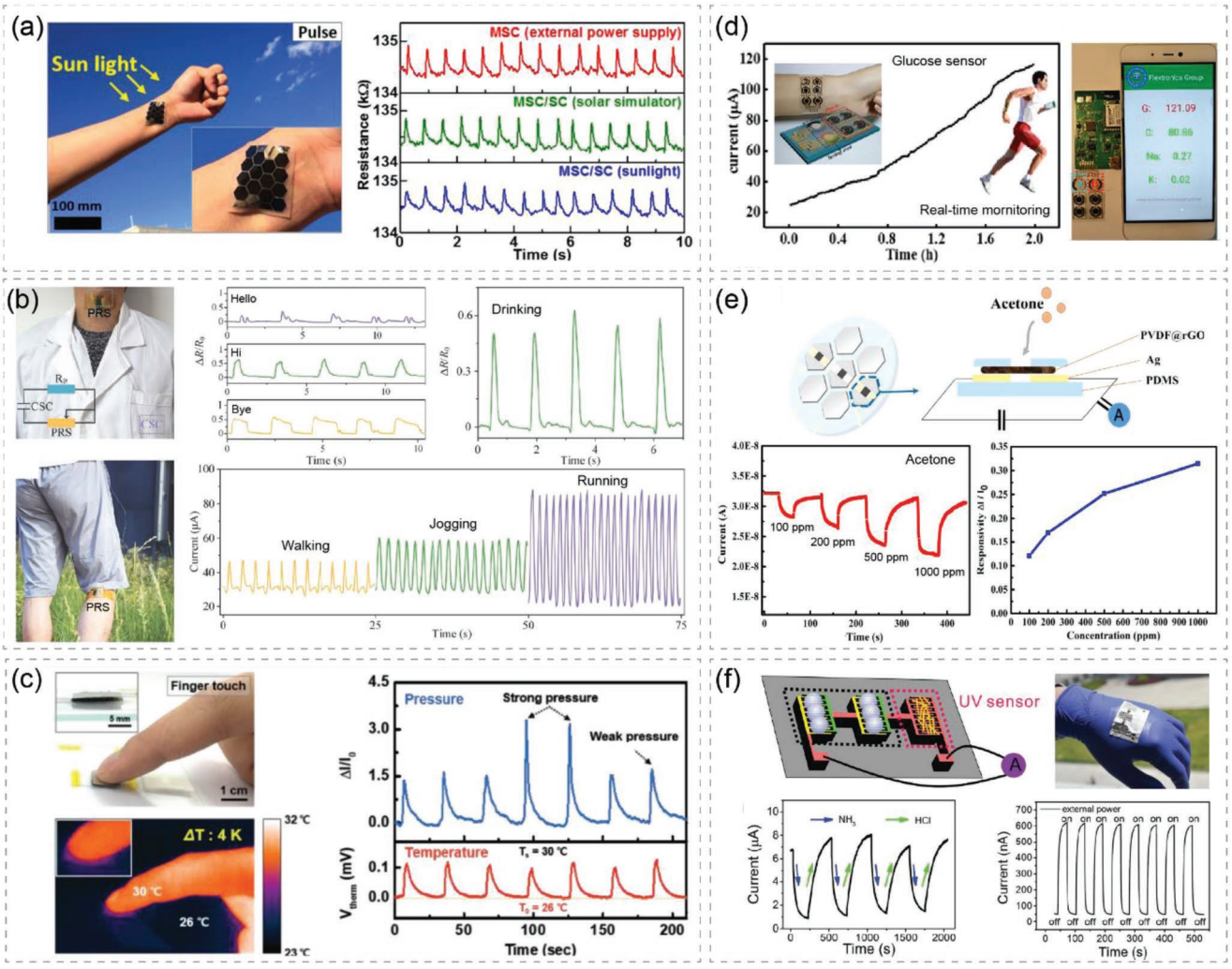

Figure 14. Two typical sensing targets of sensors powered by stretchable supercapacitors, including a–c) physical parameters and d–f) chemical parameters. a) Photograph of an integrated system attached on wrist to detect pulse signals. Reproduced with permission.[266] Copyright 2018, Elsevier Ltd. b) Photograph of a compressible system attached to the neck and leg with supercapacitor powering a pressure sensor for monitoring human motions of pronunciation, walking, jogging, and running. Reproduced with permission.[271] Copyright 2017, WILEY-VCH Verlag GmbH & Co. KGaA, Weinheim. c) Optical and thermal image of a finger touching the temperature and pressure sensor on paper. The corresponding results showed responses of a self-powered dual-mode sensor. Reproduced with permission.[272] Copyright 2018, WILEY-VCH Verlag GmbH & Co. KGaA, Weinheim. d) A $NiCo_2O_4$-based supercapacitor powering chemical sensors for the detection of chemical species in human sweat including glucose, sodium, and potassium. The real time analysis was displayed on a smart phone. Reproduced with permission.[273] Copyright 2019, Elsevier Ltd. e) Schematic illustration of an acetone sensor powered by a stretchable supercapacitor and response of the self-powered device under different acetone concentrations. Reproduced with permission.[276] Copyright 2017, Elsevier Ltd. f) Schematic illustration of a UV and gas sensor and the photograph of the device adhered onto the back of the hand. The sensors responded to gaseous NH_3 and HCl and UV illumination. Reproduced with permission.[275] Copyright 2017, WILEY-VCH Verlag GmbH & Co. KGaA, Weinheim.

of sweat with high sensitivities of 0.5 μA μM^{-1}, 0.031, and 0.056 nF mM^{-1}, respectively.[273] These information can then be transmitted to a smartphone for further analysis, as shown in Figure 14d.

Other than small molecules in solutions, various gases, such as NO_2, ethanol/acetone,[274] and NH_3/HCl[275] can also be detected by integrating sensors with stretchable supercapacitors. For instance, a NO_2 sensor operated with a biaxially stretchable supercapacitor was demonstrated, as shown in Figure 14e. The patterned-graphene sensor detected NO_2 gas when being exposed to 200 ppm NO_2 for longer than 50 min even under uniaxial stretching of 50%.

In addition, multiple sensors can be incorporated into bioelectronic devices to achieve a self-powered multiplex system. For example, Kim et al.[256] developed a stretchable multisensor powered by a wireless rechargeable microsupercapacitor array. The device could detect motions with strain sensor, UV irradiation with UV sensors, and NO_2 concentration with NO_2 gas detector. In another report, multifunctional self-powered E-skin was developed with integrated pressure sensor, photodetector, and gas sensors,[276] as shown in Figure 14f. The supercapacitor provided a stable working voltage of 0.4 V to power the sensors, which collected parameters on environmental

conditions and physiological signals. This work demonstrated the great application potential of stretchable supercapacitors in developing health monitoring bioelectronics with multiplex measurements.

5. Concluding Remarks

In summary, we have outlined the recent progress in the health monitoring applications of stretchable supercapacitor and integrated bioelectronic systems. The innovative materials for electrodes and electrolytes, including intrinsically soft and stretchable materials and structurally stretchable materials, have been the main driving factors in the development of stretchable supercapacitors. Architecture designs, such as wavy, buckled, and island-bridge patterns, are also essential for fabricating stretchable supercapacitors to conform to soft biological tissues with curved, irregular, and limited interfaces. Stretchable supercapacitors can be applied on consumer electronics, wearable bioelectronics, and implantable bioelectronics as power supplies and energy storage units. To compensate their low energy densities, they can also complement with energy harvest units, such as triboelectric devices and piezoelectric devices. For instance, soft triboelectric and piezoelectric can harvest mechanical energy generated by heart beating, which can be stored in stretchable supercapacitors for continuous power supply. These primitive integrated bioelectronic systems have shown great potential.

Overall, innovative material strategies, such as solid-state gel electrolytes, and development of new stretchable materials, such as low-dimensional crystals, have been sources of inspiration for stretchable supercapacitors with impressive electrochemical and mechanical performances. Soft, biocompatible, and biodegradable materials are representatives for developing implantable bioelectronic devices. For instance, an implantable wireless electronic device, which is made from magnesium and biodegradable polymers, can stimulate nerve system and dissolve when no longer needed,[277] and bioabsorbable and biocompatible supercapacitor has been demonstrated as energy storage units for implantable electronics.[278] These implantable bioelectronics should function robustly while immersed in physiological fluids and degrade controllably to avoid surgical removal. The mechanical property and surface affinity of the implantable bioelectronics should match with that of the biological tissue to minimize immune responses and conform to tissue movements. Adaptivity to environments and stimulus-responsiveness should also be incorporated to endow these devices with smart functionalities. Wireless function can also be designed to integrate with smart phones for monitoring and transmitting data continuously and remotely. Involving new features such as softness, biodegradability, affinity with tissues, and adaptivity, while keeping operational performance, will present critical challenges. Thus, stretchable supercapacitors and their integrated bioelectronic systems for healthcare monitoring is a growing area that needs future developments. More attempts at applying these newly developed bioelectronic systems for tackling practical issues in clinics, such as nerve healing and in vivo energy storage, are urgently needed. We envision that by transforming the conventional supercapacitors, further studies of stretchable supercapacitors as units in wearable and implantable bioelectronics can accelerate regulative approval and smooth their way into clinical applications. The advances in these systems will enable next-generation diagnostic and therapeutic systems that contribute to public health.

Acknowledgements

This work was supported by the National Natural Science Foundation of China (Grant No. 11802066), the China Postdoctoral Science Foundation (2018M633113), the Hygiene and Health Committee of Guangdong (A2019492), the Science and Technology Innovation Committee of Shenzhen (JCYJ20170818091601315), Shenzhen University Faculty Startup Grant (2019132, 2018009) and Medical Young Scientists Program, the Natural Science Foundation of Guangxi (No. 2018GXNSFBA138058), and the Guangxi Science and Technology Project (No. AD18281042). The authors are also thankful for the support from the Guangdong Province Universities, Colleges Pearl River Scholar Funded Scheme (2018), and Shenzhen Overseas High-level Talents Key Foundation for Innovation and Entrepreneurship.

Conflict of Interest

The authors declare no conflict of interest.

Keywords

energy storage, health monitoring bioelectronics, microfabrication, supercapacitors, wearable electronics

Received: August 25, 2019
Revised: November 18, 2019
Published online:

[1] M. Haghi, K. Thurow, R. Stoll, *Healthcare Inf. Res.* **2017**, *23*, 4.
[2] S. Xu, A. Jayaraman, J. A. Rogers, *Nature* **2019**, *571*, 319.
[3] D. Dias, J. Paulo Silva Cunha, *Sensors* **2018**, *18*, 2414.
[4] Y. Khan, A. E. Ostfeld, C. M. Lochner, A. Pierre, A. C. Arias, *Adv. Mater.* **2016**, *28*, 4373.
[5] B. He, Q. Zhang, L. Li, J. Sun, P. Man, Z. Zhou, Q. Li, J. Guo, L. Xie, C. Li, *J. Mater. Chem. A* **2018**, *6*, 14594.
[6] W. Gao, S. Emaminejad, H. Y. Y. Nyein, S. Challa, K. Chen, A. Peck, H. M. Fahad, H. Ota, H. Shiraki, D. Kiriya, D. H. Lien, G. A. Brooks, R. W. Davis, A. Javey, *Nature* **2016**, *529*, 509.
[7] Y. Yang, W. Gao, *Chem. Soc. Rev.* **2019**, *48*, 1465.
[8] J. D. MacKenzie, C. Ho, *Proc. IEEE* **2015**, *103*, 535.
[9] P. K. Nayak, E. M. Erickson, F. Schipper, T. R. Penki, N. Munichandraiah, P. Adelhelm, H. Sclar, F. Amalraj, B. Markovsky, D. Aurbach, *Adv. Energy Mater.* **2018**, *8*, 1702397.
[10] J. K. Kim, Y. J. Shin, L. J. Ha, D. H. Kim, D. H. Kim, *Adv. Healthcare Mater.* **2019**, *8*, 1801332.
[11] D. P. Dubal, N. R. Chodankar, D. H. Kim, P. Gomez-Romero, *Chem. Soc. Rev.* **2018**, *47*, 2065.
[12] T. An, W. Cheng, *J. Mater. Chem. A* **2018**, *6*, 15478.
[13] C. Cao, Y. Chu, Y. Zhou, C. Zhang, S. Qu, *Small* **2018**, *14*, 1803976.
[14] W. Liu, M. S. Song, B. Kong, Y. Cui, *Adv. Mater.* **2017**, *29*, 1603436.
[15] C. Zhao, Y. Liu, S. Beirne, J. Razal, J. Chen, *Adv. Mater. Technol.* **2018**, *3*, 1800028.

[16] Y. Wang, Y. Song, Y. Xia, *Chem. Soc. Rev.* **2016**, *45*, 5925.
[17] L. Wen, F. Li, H. M. Cheng, *Adv. Mater.* **2016**, *28*, 4306.
[18] A. C. Forse, C. Merlet, J. M. Griffin, C. P. Grey, *J. Am. Chem. Soc.* **2016**, *138*, 5731.
[19] J. Chmiola, G. Yushin, Y. Gogotsi, C. Portet, P. Simon, P. L. Taberna, *Science* **2006**, *313*, 1760.
[20] E. Raymundo-Pinero, K. Kierzek, J. Machnikowski, F. Béguin, *Carbon* **2006**, *44*, 2498.
[21] S. Kondrat, N. Georgi, M. V. Fedorov, A. A. Kornyshev, *Phys. Chem. Chem. Phys.* **2011**, *13*, 11359.
[22] C. Merlet, C. Péan, B. Rotenberg, P. A. Madden, B. Daffos, P. L. Taberna, P. Simon, M. Salanne, *Nat. Commun.* **2013**, *4*, 2701.
[23] D. E. Jiang, Z. Jin, J. Wu, *Nano Lett.* **2011**, *11*, 5373.
[24] F. Béguin, K. Kierzek, M. Friebe, A. Jankowska, J. Machnikowski, K. Jurewicz, E. Frackowiak, *Electrochim. Acta* **2006**, *51*, 2161.
[25] J. W. Long, D. Bélanger, T. Brousse, W. Sugimoto, M. B. Sassin, O. Crosnier, *MRS Bull.* **2011**, *36*, 513.
[26] F. Wang, X. Wu, X. Yuan, Z. Liu, Y. Zhang, L. Fu, Y. Zhu, Q. Zhou, Y. Wu, W. Huang, *Chem. Soc. Rev.* **2017**, *46*, 6816.
[27] Z. Li, X. Xue, F. Lin, Y. Wang, K. Ward, J. Fu, *Appl. Phys. Lett.* **2017**, *111*, 173105.
[28] A. M. Zamarayeva, A. E. Ostfeld, M. Wang, J. K. Duey, I. Deckman, B. P. Lechêne, G. Davies, D. A. Steingart, A. C. Arias, *Sci. Adv.* **2017**, *3*, e1602051.
[29] L. Zhang, X. Hu, Z. Wang, F. Sun, D. G. Dorrell, *Renewable Sustainable Energy Rev.* **2018**, *81*, 1868.
[30] G. F. L. Pereira, R. G. Pereira, M. Salanne, L. J. A. Siqueira, *J. Phys. Chem. C* **2019**, *123*, 10816.
[31] W. Zilong, Z. Zhu, J. Qiu, S. Yang, *J. Mater. Chem. C* **2014**, *2*, 1331.
[32] A. Muzaffar, M. B. Ahamed, K. Deshmukh, J. Thirumalai, *Renewable Sustainable Energy Rev.* **2019**, *101*, 123.
[33] A. González, E. Goikolea, J. A. Barrena, R. Mysyk, *Renewable Sustainable Energy Rev.* **2016**, *58*, 1189.
[34] K. Jost, D. Stenger, C. R. Perez, J. K. McDonough, K. Lian, Y. Gogotsi, G. Dion, *Energy Environ. Sci.* **2013**, *6*, 2698.
[35] J. Zang, C. Cao, Y. Feng, J. Liu, X. Zhao, *Sci. Rep.* **2015**, *4*, 6492.
[36] P. Xu, J. Kang, J. B. Choi, J. Suhr, J. Yu, F. Li, J. H. Byun, B. S. Kim, T. W. Chou, *ACS Nano* **2014**, *8*, 9437.
[37] R. Cruz-Silva, A. Morelos-Gomez, H. I. Kim, H. K. Jang, F. Tristan, S. Vega-Diaz, L. P. Rajukumar, A. L. Elías, N. Perea-Lopez, J. Suhr, *ACS Nano* **2014**, *8*, 5959.
[38] T. Chen, Y. Xue, A. K. Roy, L. Dai, *ACS Nano* **2014**, *8*, 1039.
[39] Y. Meng, Y. Zhao, C. Hu, H. Cheng, Y. Hu, Z. Zhang, G. Shi, L. Qu, *Adv. Mater.* **2013**, *25*, 2326.
[40] Z. Lv, Y. Tang, Z. Zhu, J. Wei, W. Li, H. Xia, Y. Jiang, Z. Liu, Y. Luo, X. Ge, *Adv. Mater.* **2018**, *30*, 1805468.
[41] X. Liang, L. Zhao, Q. Wang, Y. Ma, D. Zhang, *Nanoscale* **2018**, *10*, 22329.
[42] T. Lv, Y. Yao, N. Li, T. Chen, *Angew. Chem., Int. Ed.* **2016**, *55*, 9191.
[43] N. Li, T. Lv, Y. Yao, H. Li, K. Liu, T. Chen, *J. Mater. Chem. A* **2017**, *5*, 3267.
[44] T. Gu, B. Wei, *J. Mater. Chem. A* **2016**, *4*, 12289.
[45] Y. Shi, L. Peng, Y. Ding, Y. Zhao, G. Yu, *Chem. Soc. Rev.* **2015**, *44*, 6684.
[46] Y. Wang, Y. Ding, X. Guo, G. Yu, *Nano Res.* **2019**, *12*, 1978.
[47] Y. Zhou, X. Wang, L. Acauan, E. Kalfon-Cohen, X. Ni, Y. Stein, K. K. Gleason, B. L. Wardle, *Adv. Mater.* **2019**, *31*, 1901916.
[48] C. R. Chen, H. Qin, H. P. Cong, S. H. Yu, *Adv. Mater.* **2019**, *31*, 1900573.
[49] H. Jiang, Z. Wang, Q. Yang, M. Hanif, Z. Wang, L. Dong, M. Dong, *Electrochim. Acta* **2018**, *290*, 695.
[50] K. Zhao, H. Wang, C. Zhu, S. Lin, Z. Xu, X. Zhang, *Electrochim. Acta* **2019**, *308*, 1.
[51] M. Guo, C. Liu, Z. Zhang, J. Zhou, Y. Tang, S. Luo, *Adv. Funct. Mater.* **2018**, *28*, 1803196.
[52] M. Naguib, M. Kurtoglu, V. Presser, J. Lu, J. Niu, M. Heon, L. Hultman, Y. Gogotsi, M. W. Barsoum, *Adv. Mater.* **2011**, *23*, 4248.
[53] H. Liao, X. Guo, P. Wan, G. Yu, *Adv. Funct. Mater.* **2019**, *29*, 1904507.
[54] J. Zhou, J. Yu, L. Shi, Z. Wang, H. Liu, B. Yang, C. Li, C. Zhu, J. Xu, *Small* **2018**, *14*, 1803786.
[55] Y. Yue, N. Liu, Y. Ma, S. Wang, W. Liu, C. Luo, H. Zhang, F. Cheng, J. Rao, X. Hu, *ACS Nano* **2018**, *12*, 4224.
[56] Z. Fan, Y. Wang, Z. Xie, X. Xu, Y. Yuan, Z. Cheng, Y. Liu, *Nanoscale* **2018**, *10*, 9642.
[57] H. N. Wang, M. Zhang, A. M. Zhang, F. C. Shen, X. K. Wang, S. N. Sun, Y. J. Chen, Y. Q. Lan, *ACS Appl. Mater. Interfaces* **2018**, *10*, 32265.
[58] W. Zhao, J. Peng, W. Wang, B. Jin, T. Chen, S. Liu, Q. Zhao, W. Huang, *Small* **2019**, *15*, 1901351.
[59] D. Sheberla, J. C. Bachman, J. S. Elias, C. J. Sun, Y. Shao-Horn, M. Dincă, *Nat. Mater.* **2017**, *16*, 220.
[60] X. M. Cao, Z. B. Han, *Chem. Commun.* **2019**, *55*, 1746.
[61] H. Wu, W. Zhang, S. Kandambeth, O. Shekhah, M. Eddaoudi, H. N. Alshareef, *Adv. Energy Mater.* **2019**, *9*, 1900482.
[62] Y. Chen, M. Han, Y. Tang, J. Bao, S. Li, Y. Lan, Z. Dai, *Chem. Commun.* **2015**, *51*, 12377.
[63] B. Yang, C. Hao, F. Wen, B. Wang, C. Mu, J. Xiang, L. Li, B. Xu, Z. Zhao, Z. Liu, *ACS Appl. Mater. Interfaces* **2017**, *9*, 44478.
[64] X. Y. Fu, Z. D. Chen, Y. L. Zhang, D. D. Han, J. N. Ma, W. Wang, Z. R. Zhang, H. Xia, H. B. Sun, *Nanoscale* **2019**, *11*, 9133.
[65] S. Luo, J. Zhao, J. Zou, Z. He, C. Xu, F. Liu, Y. Huang, L. Dong, L. Wang, H. Zhang, *ACS Appl. Mater. Interfaces* **2018**, *10*, 3538.
[66] X. Wu, Y. Xu, Y. Hu, G. Wu, H. Cheng, Q. Yu, K. Zhang, W. Chen, S. Chen, *Nat. Commun.* **2018**, *9*, 4573.
[67] X. Lu, M. Yu, G. Wang, Y. Tong, Y. Li, *Energy Environ. Sci.* **2014**, *7*, 2160.
[68] L. Zhang, D. DeArmond, N. T. Alvarez, R. Malik, N. Oslin, C. McConnell, P. K. Adusei, Y. Y. Hsieh, V. Shanov, *Small* **2017**, *13*, 1603114.
[69] C. J. Zhang, T. M. Higgins, S. H. Park, S. E. O'Brien, D. Long, J. N. Coleman, V. Nicolosi, *Nano Energy* **2016**, *28*, 495.
[70] I. M. Mosa, A. Pattammattel, K. Kadimisetty, P. Pande, M. F. El-Kady, G. W. Bishop, M. Novak, R. B. Kaner, A. K. Basu, C. V. Kumar, J. F. Rusling, *Adv. Energy Mater.* **2017**, *7*, 1700358.
[71] E. Eustache, C. Douard, R. Retoux, C. Lethien, T. Brousse, *Adv. Energy Mater.* **2015**, *5*, 1500680.
[72] J. Lv, I. Jeerapan, F. Tehrani, L. Yin, C. A. Silva-Lopez, J. H. Jang, D. Joshuia, R. Shah, Y. Liang, L. Xie, *Energy Environ. Sci.* **2018**, *11*, 3431.
[73] Z. Y. Jin, A. H. Lu, Y. Y. Xu, J. T. Zhang, W. C. Li, *Adv. Mater.* **2014**, *26*, 3700.
[74] S. He, Y. Hu, J. Wan, Q. Gao, Y. Wang, S. Xie, L. Qiu, C. Wang, G. Zheng, B. Wang, *Carbon* **2017**, *122*, 162.
[75] J. S. Chae, N. S. Heo, C. H. Kwak, W. S. Cho, G. H. Seol, W. S. Yoon, H. K. Kim, D. J. Fray, A. T. E. Vilian, Y. K. Han, *Nano Energy* **2017**, *34*, 86.
[76] Z. Lu, J. Foroughi, C. Wang, H. Long, G. G. Wallace, *Adv. Energy Mater.* **2018**, *8*, 1702047.
[77] C. Zhao, C. Wang, Z. Yue, K. Shu, G. G. Wallace, *ACS Appl. Mater. Interfaces* **2013**, *5*, 9008.
[78] D. Kim, G. Lee, D. Kim, J. Yun, S. S. Lee, J. S. Ha, *Nanoscale* **2016**, *8*, 15611.
[79] B. Pal, A. Yasin, R. Kunwar, S. Yang, M. M. Yusoff, R. Jose, *Ind. Eng. Chem. Res.* **2018**, *58*, 654.
[80] Y. Lin, H. Zhang, H. Liao, Y. Zhao, K. Li, *Chem. Eng. J.* **2019**, *367*, 139.
[81] L. Liu, Y. Yu, C. Yan, K. Li, Z. Zheng, *Nat. Commun.* **2015**, *6*, 7260.
[82] J. Xie, X. Sun, N. Zhang, K. Xu, M. Zhou, Y. Xie, *Nano Energy* **2013**, *2*, 65.

[83] B. Wang, X. Fang, H. Sun, S. He, J. Ren, Y. Zhang, H. Peng, *Adv. Mater.* **2015**, *27*, 7854.
[84] Y. J. Kang, Y. Yoo, W. Kim, *ACS Appl. Mater. Interfaces* **2016**, *8*, 13909.
[85] J. Q. Xie, Y. Q. Ji, J. H. Kang, J. L. Sheng, D. S. Mao, X. Z. Fu, R. Sun, C. P. Wong, *Energy Environ. Sci.* **2019**, *12*, 194.
[86] L. Feng, K. Wang, X. Zhang, X. Sun, C. Li, X. Ge, Y. Ma, *Adv. Funct. Mater.* **2018**, *28*, 1704463.
[87] X. Zhang, M. Kar, T. C. Mendes, Y. Wu, D. R. MacFarlane, *Adv. Energy Mater.* **2018**, *8*, 1702702.
[88] Y. Yue, N. Liu, Y. Ma, S. Wang, W. Liu, C. Luo, H. Zhang, F. Cheng, J. Rao, X. Hu, J. Su, Y. Gao, *ACS Nano* **2018**, *12*, 4224.
[89] S. Wang, N. Liu, J. Su, L. Li, F. Long, Z. Zou, X. Jiang, Y. Gao, *ACS Nano* **2017**, *11*, 2066.
[90] Y. Guo, J. Bae, F. Zhao, G. Yu, *Trends Chem.* **2019**, *1*, 335.
[91] P. Li, Z. Jin, L. Peng, F. Zhao, D. Xiao, Y. Jin, G. Yu, *Adv. Mater.* **2018**, *30*, 1800124.
[92] T. Chen, H. Peng, M. Durstock, L. Dai, *Sci. Rep.* **2015**, *4*, 3612.
[93] Y. Huang, M. Zhong, Y. Huang, M. Zhu, Z. Pei, Z. Wang, Q. Xue, X. Xie, C. Zhi, *Nat. Commun.* **2015**, *6*, 10310.
[94] Y. Wang, F. Chen, Z. Liu, Z. Tang, Q. Yang, Y. Zhao, S. Du, Q. Chen, C. Zhi, *Angew. Chem., Int. Ed.* **2019**, *131*, 15854.
[95] D. Chen, K. Jiang, T. Huang, G. Shen, *Adv. Mater.* **2019**, 1901806, https://onlinelibrary.wiley.com/doi/abs/10.1002/adma.201901806.
[96] D. Yu, Q. Qian, L. Wei, W. Jiang, K. Goh, J. Wei, J. Zhang, Y. Chen, *Chem. Soc. Rev.* **2015**, *44*, 647.
[97] A. Sumboja, J. Liu, W. G. Zheng, Y. Zong, H. Zhang, Z. Liu, *Chem. Soc. Rev.* **2018**, *47*, 5919.
[98] F. M. Guo, R. Q. Xu, X. Cui, L. Zhang, K. L. Wang, Y. W. Yao, J. Q. Wei, *J. Mater. Chem. A* **2016**, *4*, 9311.
[99] C. Choi, S. H. Kim, H. J. Sim, J. A. Lee, A. Y. Choi, Y. T. Kim, X. Lepró, G. M. Spinks, R. H. Baughman, S. J. Kim, *Sci. Rep.* **2015**, *5*, 9387.
[100] M. Li, M. Zu, J. Yu, H. Cheng, Q. Li, *Small* **2017**, *13*, 1602994.
[101] T. Chen, R. Hao, H. Peng, L. Dai, *Angew. Chem., Int. Ed.* **2015**, *54*, 618.
[102] J. Yu, M. Wang, P. Xu, S. H. Cho, J. Suhr, K. Gong, L. Meng, Y. Huang, J. H. Byun, Y. Oh, *Carbon* **2017**, *119*, 332.
[103] C. Choi, K. M. Kim, K. J. Kim, X. Lepró, G. M. Spinks, R. H. Baughman, S. J. Kim, *Nat. Commun.* **2016**, *7*, 13811.
[104] K. Qi, R. Hou, S. Zaman, Y. Qiu, B. Y. Xia, H. Duan, *ACS Appl. Mater. Interfaces* **2018**, *10*, 18021.
[105] B. S. Kim, K. Lee, S. Kang, S. Lee, J. B. Pyo, I. S. Choi, K. Char, J. H. Park, S. S. Lee, J. Lee, *Nanoscale* **2017**, *9*, 13272.
[106] D. Yu, S. Zhai, W. Jiang, K. Goh, L. Wei, X. Chen, R. Jiang, Y. Chen, *Adv. Mater.* **2015**, *27*, 4895.
[107] C. Choi, J. M. Lee, S. H. Kim, S. J. Kim, J. Di, R. H. Baughman, *Nano Lett.* **2016**, *16*, 7677.
[108] C. Choi, J. H. Kim, H. J. Sim, J. Di, R. H. Baughman, S. J. Kim, *Adv. Energy Mater.* **2017**, *7*, 1602021.
[109] X. Chen, H. Lin, J. Deng, Y. Zhang, X. Sun, P. Chen, X. Fang, Z. Zhang, G. Guan, H. Peng, *Adv. Mater.* **2014**, *26*, 8126.
[110] Y. Huang, M. Zhu, Z. Pei, Q. Xue, Y. Huang, C. Zhi, *J. Mater. Chem. A* **2016**, *4*, 1290.
[111] Z. Zhang, J. Deng, X. Li, Z. Yang, S. He, X. Chen, G. Guan, J. Ren, H. Peng, *Adv. Mater.* **2015**, *27*, 356.
[112] Z. Zhang, L. Wang, Y. Li, Y. Wang, J. Zhang, G. Guan, Z. Pan, G. Zheng, H. Peng, *Adv. Energy Mater.* **2017**, *7*, 1601814.
[113] Z. Yang, J. Deng, X. Chen, J. Ren, H. Peng, *Angew. Chem., Int. Ed.* **2013**, *52*, 13453.
[114] H. Wang, Z. Liu, J. Ding, X. Lepró, S. Fang, N. Jiang, N. Yuan, R. Wang, Q. Yin, W. Lv, *Adv. Mater.* **2016**, *28*, 4998.
[115] L. Liu, W. Ma, Z. Zhang, *Small* **2011**, *7*, 1504.
[116] S. J. Kim, M. A. Kang, I. S. Jeon, S. Ji, W. Song, S. Myung, S. S. Lee, J. Lim, K. S. An, *J. Mater. Chem. C* **2017**, *5*, 12354.
[117] G. Sun, X. Zhang, R. Lin, J. Yang, H. Zhang, P. Chen, *Angew. Chem., Int. Ed.* **2015**, *54*, 4651.
[118] W. Xu, S. Dai, G. Liu, Y. Xi, C. Hu, X. Wang, *Electrochim. Acta* **2016**, *203*, 1.
[119] Y. Huang, H. Hu, Y. Huang, M. Zhu, W. Meng, C. Liu, Z. Pei, C. Hao, Z. Wang, C. Zhi, *ACS Nano* **2015**, *9*, 4766.
[120] L. Kou, T. Huang, B. Zheng, Y. Han, X. Zhao, K. Gopalsamy, H. Sun, C. Gao, *Nat. Commun.* **2014**, *5*, 3754.
[121] S. Cai, T. Huang, H. Chen, M. Salman, K. Gopalsamy, C. Gao, *J. Mater. Chem. A* **2017**, *5*, 22489.
[122] L. Kou, Z. Liu, T. Huang, B. Zheng, Z. Tian, Z. Deng, C. Gao, *Nanoscale* **2015**, *7*, 4080.
[123] K. Jiang, J. Wang, Q. Li, L. Liu, C. Liu, S. Fan, *Adv. Mater.* **2011**, *23*, 1154.
[124] Z. Zhang, D. Zhang, H. Lin, Y. Chen, *J. Power Sources* **2019**, *433*, 226711.
[125] X. Wu, G. Wu, P. Tan, H. Cheng, R. Hong, F. Wang, S. Chen, *J. Mater. Chem. A* **2018**, *6*, 8940.
[126] Y. L. Tong, B. Xu, X. F. Du, H. Y. Cheng, C. F. Wang, G. Wu, S. Chen, *Macromol. Mater. Eng.* **2018**, *303*, 1700664.
[127] H. Pan, D. Wang, Q. Peng, J. Ma, X. Meng, Y. Zhang, Y. Ma, S. Zhu, D. Zhang, *ACS Appl. Mater. Interfaces* **2018**, *10*, 10157.
[128] G. Wu, P. Tan, X. Wu, L. Peng, H. Cheng, C. F. Wang, W. Chen, Z. Yu, S. Chen, *Adv. Funct. Mater.* **2017**, *27*, 1702493.
[129] C. Yu, C. Masarapu, J. Rong, B. Wei, H. Jiang, *Adv. Mater.* **2009**, *21*, 4793.
[130] Y. Xie, Y. Liu, Y. Zhao, Y. H. Tsang, S. P. Lau, H. Huang, Y. Chai, *J. Mater. Chem. A* **2014**, *2*, 9142.
[131] X. Li, T. Gu, B. Wei, *Nano Lett.* **2012**, *12*, 6366.
[132] Y. Huang, M. Zhong, F. Shi, X. Liu, Z. Tang, Y. Wang, Y. Huang, H. Hou, X. Xie, C. Zhi, *Angew. Chem., Int. Ed.* **2017**, *56*, 9141.
[133] K. J. Kim, J. A. Lee, M. D. Lima, R. H. Baughman, S. J. Kim, *RSC Adv.* **2016**, *6*, 24756.
[134] A. Ferris, D. Bourrier, S. Garbarino, D. Guay, D. Pech, *Small* **2019**, *15*, 1901224.
[135] J. H. Sung, S. J. Kim, K. H. Lee, *J. Power Sources* **2004**, *133*, 312.
[136] F. Li, J. Chen, X. Wang, M. Xue, G. F. Chen, *Adv. Funct. Mater.* **2015**, *25*, 4601.
[137] L. Li, Z. Lou, W. Han, D. Chen, K. Jiang, G. Shen, *Adv. Mater. Technol.* **2017**, *2*, 1600282.
[138] D. Kim, G. Shin, Y. J. Kang, W. Kim, J. S. Ha, *ACS Nano* **2013**, *7*, 7975.
[139] J. Yun, Y. Lim, H. Lee, G. Lee, H. Park, S. Y. Hong, S. W. Jin, Y. H. Lee, S. S. Lee, J. S. Ha, *Adv. Funct. Mater.* **2017**, *27*, 1700135.
[140] Y. Lim, J. Yoon, J. Yun, D. Kim, S. Y. Hong, S. J. Lee, G. Zi, J. S. Ha, *ACS Nano* **2014**, *8*, 11639.
[141] K. Robert, C. Douard, A. Demortière, F. Blanchard, P. Roussel, T. Brousse, C. Lethien, *Adv. Mater. Technol.* **2018**, *3*, 1800036.
[142] T. Cheng, Y. Z. Zhang, J. D. Zhang, W. Y. Lai, W. Huang, *J. Mater. Chem. A* **2016**, *4*, 10493.
[143] Q. Wu, J. Wei, B. Xu, X. Liu, H. Wang, W. Wang, Q. Wang, W. Liu, *Sci. Rep.* **2017**, *7*, 41566.
[144] Z. S. Wu, K. Parvez, X. Feng, K. Müllen, *J. Mater. Chem. A* **2014**, *2*, 8288.
[145] L. Wang, D. Wang, X. Y. Dong, Z. J. Zhang, X. F. Pei, X. J. Chen, B. Chen, J. Jin, *Chem. Commun.* **2011**, *47*, 3556.
[146] D. Aradilla, D. Gaboriau, G. Bidan, P. Gentile, M. Boniface, D. Dubal, P. Gómez-Romero, J. Wimberg, T. J. S. Schubert, S. Sadki, *J. Mater. Chem. A* **2015**, *3*, 13978.
[147] L. Cao, S. Yang, W. Gao, Z. Liu, Y. Gong, L. Ma, G. Shi, S. Lei, Y. Zhang, S. Zhang, *Small* **2013**, *9*, 2905.
[148] A. Lamberti, F. Clerici, M. Fontana, L. Scaltrito, *Adv. Energy Mater.* **2016**, *6*, 1600050.
[149] E. Eustache, C. Douard, A. Demortière, V. De Andrade, M. Brachet, J. Le Bideau, T. Brousse, C. Lethien, *Adv. Mater. Technol.* **2017**, *2*, 1700126.

[150] N. Kurra, Q. Jiang, H. N. Alshareef, *Nano Energy* **2015**, *16*, 1.
[151] M. F. El-Kady, R. B. Kaner, *Nat. Commun.* **2013**, *4*, 1475.
[152] M. Xue, Z. Xie, L. Zhang, X. Ma, X. Wu, Y. Guo, W. Song, Z. Li, T. Cao, *Nanoscale* **2011**, *3*, 2703.
[153] C. Lethien, J. Le Bideau, T. Brousse, *Energy Environ. Sci.* **2019**, *12*, 96.
[154] J. Maeng, Y. J. Kim, C. Meng, P. P. Irazoqui, *ACS Appl. Mater. Interfaces* **2016**, *8*, 13458.
[155] S. Nardecchia, D. Carriazo, M. L. Ferrer, M. C. Gutiérrez, F. del Monte, *Chem. Soc. Rev.* **2013**, *42*, 794.
[156] K. Olszowska, J. Pang, P. S. Wrobel, L. Zhao, H. Q. Ta, Z. Liu, B. Trzebicka, A. Bachmatiuk, M. H. Rummeli, *Synth. Met.* **2017**, *234*, 53.
[157] S. Zhai, H. E. Karahan, L. Wei, Q. Qian, A. T. Harris, A. I. Minett, S. Ramakrishna, A. K. Ng, Y. Chen, *Energy Storage Mater.* **2016**, *3*, 123.
[158] S. Jiao, A. Zhou, M. Wu, H. Hu, *Adv. Sci.* **2019**, *6*, 1900529.
[159] S. He, L. Qiu, L. Wang, J. Cao, S. Xie, Q. Gao, Z. Zhang, J. Zhang, B. Wang, H. Peng, *J. Mater. Chem. A* **2016**, *4*, 14968.
[160] R. Xu, A. Zverev, A. Hung, C. Shen, L. Irie, G. Ding, M. Whitmeyer, L. Ren, B. Griffin, J. Melcher, *Microsyst. Nanoeng.* **2018**, *4*, 36.
[161] Z. Lv, Y. Luo, Y. Tang, J. Wei, Z. Zhu, X. Zhou, W. Li, Y. Zeng, W. Zhang, Y. Zhang, *Adv. Mater.* **2018**, *30*, 1704531.
[162] I. Nam, G. P. Kim, S. Park, J. W. Han, J. Yi, *Energy Environ. Sci.* **2014**, *7*, 1095.
[163] S. He, J. Cao, S. Xie, J. Deng, Q. Gao, L. Qiu, J. Zhang, L. Wang, Y. Hu, H. Peng, *J. Mater. Chem. A* **2016**, *4*, 10124.
[164] Z. Niu, W. Zhou, X. Chen, J. Chen, S. Xie, *Adv. Mater.* **2015**, *27*, 6002.
[165] X. L. Wu, T. Wen, H. L. Guo, S. Yang, X. Wang, A. W. Xu, *ACS Nano* **2013**, *7*, 3589.
[166] X. Yu, X. Su, K. Yan, H. Hu, M. Peng, X. Cai, D. Zou, *Adv. Mater. Technol.* **2016**, *1*, 1600009.
[167] L. Hu, M. Pasta, F. La Mantia, L. Cui, S. Jeong, H. D. Deshazer, J. W. Choi, S. M. Han, Y. Cui, *Nano Lett.* **2010**, *10*, 708.
[168] U. Gulzar, S. Goriparti, E. Miele, T. Li, G. Maidecchi, A. Toma, F. De Angelis, C. Capiglia, R. P. Zaccaria, *J. Mater. Chem. A* **2016**, *4*, 16771.
[169] Y. H. Lee, Y. Kim, T. I. Lee, I. Lee, J. Shin, H. S. Lee, T. S. Kim, J. W. Choi, *ACS Nano* **2015**, *9*, 12214.
[170] X. Gui, J. Wei, K. Wang, A. Cao, H. Zhu, Y. Jia, Q. Shu, D. Wu, *Adv. Mater.* **2010**, *22*, 617.
[171] Z. Li, K. Hu, M. Yang, Y. Zou, J. Yang, M. Yu, H. Wang, X. Qu, P. Tan, C. Wang, *Nano Energy* **2019**, *58*, 852.
[172] Z. Fan, Y. Liu, J. Yan, G. Ning, Q. Wang, T. Wei, L. Zhi, F. Wei, *Adv. Energy Mater.* **2012**, *2*, 419.
[173] D. P. Dubal, D. Aradilla, G. Bidan, P. Gentile, T. J. S. Schubert, J. Wimberg, S. Sadki, P. Gomez-Romero, *Sci. Rep.* **2015**, *5*, 9771.
[174] K. Gerasopoulos, E. Pomerantseva, M. McCarthy, A. Brown, C. Wang, J. Culver, R. Ghodssi, *ACS Nano* **2012**, *6*, 6422.
[175] J. Y. Hong, B. M. Bak, J. J. Wie, J. Kong, H. S. Park, *Adv. Funct. Mater.* **2015**, *25*, 1053.
[176] B. G. Choi, M. Yang, W. H. Hong, J. W. Choi, Y. S. Huh, *ACS Nano* **2012**, *6*, 4020.
[177] Q. Huang, D. Wang, Z. Zheng, *Adv. Energy Mater.* **2016**, *6*, 1600783.
[178] Y. Ai, Z. Lou, L. Li, S. Chen, H. S. Park, Z. M. Wang, G. Shen, *Adv. Mater. Technol.* **2016**, *1*, 1600142.
[179] S. W. Zhang, B. S. Yin, C. Liu, Z. B. Wang, D. M. Gu, *J. Mater. Chem. A* **2017**, *5*, 15144.
[180] Y. Chen, B. Xu, J. Wen, J. Gong, T. Hua, C. W. Kan, J. Deng, *Small* **2018**, *14*, 1704373.
[181] J. Sun, Y. Huang, C. Fu, Z. Wang, Y. Huang, M. Zhu, C. Zhi, H. Hu, *Nano Energy* **2016**, *27*, 230.
[182] S. S. Lee, K. H. Choi, S. H. Kim, S. Y. Lee, *Adv. Funct. Mater.* **2018**, *28*, 1705571.
[183] F. Yi, J. Wang, X. Wang, S. Niu, S. Li, Q. Liao, Y. Xu, Z. You, Y. Zhang, Z. L. Wang, *ACS Nano* **2016**, *10*, 6519.
[184] B. Xie, C. Yang, Z. Zhang, P. Zou, Z. Lin, G. Shi, Q. Yang, F. Kang, C. P. Wong, *ACS Nano* **2015**, *9*, 5636.
[185] H. Jin, L. Zhou, C. L. Mak, H. Huang, W. M. Tang, H. L. W. Chan, *Nano Energy* **2015**, *11*, 662.
[186] Y. Zhao, D. Dong, Y. Wang, S. Gong, T. An, L. W. Yap, W. Cheng, *ACS Appl. Mater. Interfaces* **2018**, *10*, 42612.
[187] N. Zhang, W. Zhou, Q. Zhang, P. Luan, L. Cai, F. Yang, X. Zhang, Q. Fan, W. Zhou, Z. Xiao, *Nanoscale* **2015**, *7*, 12492.
[188] J. Pu, X. Wang, R. Xu, K. Komvopoulos, *ACS Nano* **2016**, *10*, 9306.
[189] D. Shin, C. Shen, M. Sanghadasa, L. Lin, *Adv. Mater. Technol.* **2018**, *3*, 1800209.
[190] C. Shen, Y. Xie, B. Zhu, M. Sanghadasa, Y. Tang, L. Lin, *Sci. Rep.* **2017**, *7*, 14324.
[191] Z. Song, Y. Fan, Z. Sun, D. Han, Y. Bao, L. Niu, *J. Mater. Chem. A* **2017**, *5*, 20797.
[192] T. G. Yun, M. Park, D. H. Kim, D. Kim, J. Y. Cheong, J. G. Bae, S. M. Han, I. D. Kim, *ACS Nano* **2019**, *13*, 3141.
[193] H. Kim, J. Yoon, G. Lee, S. H. Paik, G. Choi, D. Kim, B. M. Kim, G. Zi, J. S. Ha, *ACS Appl. Mater. Interfaces* **2016**, *8*, 16016.
[194] W. Song, J. Zhu, B. Gan, S. Zhao, H. Wang, C. Li, J. Wang, *Small* **2018**, *14*, 1702249.
[195] S. Zhu, Y. Li, H. Zhu, J. Ni, Y. Li, *Small* **2019**, *15*, 1804037.
[196] G. Lee, D. Kim, D. Kim, S. Oh, J. Yun, J. Kim, S. S. Lee, J. S. Ha, *Energy Environ. Sci.* **2015**, *8*, 1764.
[197] P. Luan, N. Zhang, W. Zhou, Z. Niu, Q. Zhang, L. Cai, X. Zhang, F. Yang, Q. Fan, W. Zhou, *Adv. Funct. Mater.* **2016**, *26*, 8178.
[198] G. Lee, J. W. Kim, H. Park, J. Y. Lee, H. Lee, C. Song, S. W. Jin, K. Keum, C. H. Lee, J. S. Ha, *ACS Nano* **2019**, *13*, 855.
[199] Z. Liu, Z. S. Wu, S. Yang, R. Dong, X. Feng, K. Müllen, *Adv. Mater.* **2016**, *28*, 2217.
[200] T. An, Y. Ling, S. Gong, B. Zhu, Y. Zhao, D. Dong, L. W. Yap, Y. Wang, W. Cheng, *Adv. Mater. Technol.* **2019**, *4*, 1800473.
[201] G. Lee, S. K. Kang, S. M. Won, P. Gutruf, Y. R. Jeong, J. Koo, S. S. Lee, J. A. Rogers, J. S. Ha, *Adv. Energy Mater.* **2017**, *7*, 1700157.
[202] S. Gong, W. Cheng, *Adv. Energy Mater.* **2017**, *7*, 1700648.
[203] P. Song, S. Kuang, N. Panwar, G. Yang, D. J. H. Tng, S. C. Tjin, W. J. Ng, M. B. A. Majid, G. Zhu, K. T. Yong, *Adv. Mater.* **2017**, *29*, 1605668.
[204] J. A. Potkay, *Biomed. Microdevices* **2008**, *10*, 379.
[205] I. E. Araci, B. Su, S. R. Quake, Y. Mandel, *Nat. Med.* **2014**, *20*, 1074.
[206] Q. Zheng, B. Shi, F. Fan, X. Wang, L. Yan, W. Yuan, S. Wang, H. Liu, Z. Li, Z. L. Wang, *Adv. Mater.* **2014**, *26*, 5851.
[207] A. Lamberti, C. F. Pirri, *J. Energy Storage* **2016**, *8*, 193.
[208] W. Jiang, H. Li, Z. Liu, Z. Li, J. Tian, B. Shi, Y. Zou, H. Ouyang, C. Zhao, L. Zhao, *Adv. Mater.* **2018**, *30*, 1801895.
[209] M. G. Saborio, Š. Zukić, S. Lanzalaco, J. Casanovas, J. Puiggali, F. Estrany, C. Aleman, *Mater. Today Commun.* **2018**, *16*, 60.
[210] C. A. Amarnath, N. Venkatesan, M. Doble, S. N. Sawant, *J. Mater. Chem. B* **2014**, *2*, 5012.
[211] N. Sattarahmady, R. D. Vais, H. Heli, *J. Appl. Electrochem.* **2015**, *45*, 577.
[212] C. Meng, O. Z. Gall, P. P. Irazoqui, *Biomed. Microdevices* **2013**, *15*, 973.
[213] S. R. Shin, C. K. Lee, I. S. So, J. H. Jeon, T. M. Kang, C. W. Kee, S. I. Kim, G. M. Spinks, G. G. Wallace, S. J. Kim, *Adv. Mater.* **2008**, *20*, 466.
[214] Y. J. Kang, S. J. Chun, S. S. Lee, B. Y. Kim, J. H. Kim, H. Chung, S. Y. Lee, W. Kim, *ACS Nano* **2012**, *6*, 6400.
[215] N. Sattarahmady, A. Parsa, H. Heli, *J. Mater. Sci.* **2013**, *48*, 2346.
[216] T. Bobrowski, E. G. Arribas, R. Ludwig, M. D. Toscano, S. Shleev, W. Schuhmann, *Biosens. Bioelectron.* **2018**, *101*, 84.

[217] M. Salari, S. H. Aboutalebi, I. Ekladious, R. Jalili, K. Konstantinov, H. K. Liu, M. W. Grinstaff, *Adv. Mater. Technol.* **2018**, *3*, 1700194.
[218] K. Hu, R. Xiong, H. Guo, R. Ma, S. Zhang, Z. L. Wang, V. V. Tsukruk, *Adv. Mater.* **2016**, *28*, 3549.
[219] H. J. Sim, C. Choi, D. Y. Lee, H. Kim, J. H. Yun, J. M. Kim, T. M. Kang, R. Ovalle, R. H. Baughman, C. W. Kee, *Nano Energy* **2018**, *47*, 385.
[220] O. Z. Gall, C. Meng, H. Bhamra, H. Mei, S. W. M. John, P. P. Irazoqui, *Circuits, Syst. Signal Process.* **2019**, *38*, 1360.
[221] Y. Ma, Q. Zheng, Y. Liu, B. Shi, X. Xue, W. Ji, Z. Liu, Y. Jin, Y. Zou, Z. An, *Nano Lett.* **2016**, *16*, 6042.
[222] B. Shi, Z. Li, Y. Fan, *Adv. Mater.* **2018**, *30*, 1801511.
[223] Q. Zheng, Y. Zou, Y. Zhang, Z. Liu, B. Shi, X. Wang, Y. Jin, H. Ouyang, Z. Li, Z. L. Wang, *Sci. Adv.* **2016**, *2*, e1501478.
[224] H. Ouyang, Z. Liu, N. Li, B. Shi, Y. Zou, F. Xie, Y. Ma, Z. Li, H. Li, Q. Zheng, *Nat. Commun.* **2019**, *10*, 1821.
[225] B. Shi, Z. Liu, Q. Zheng, J. Meng, H. Ouyang, Y. Zou, D. Jiang, X. Qu, M. Yu, L. Zhao, *ACS Nano* **2019**, *13*, 6017.
[226] Y. Zou, P. Tan, B. Shi, H. Ouyang, D. Jiang, Z. Liu, H. Li, M. Yu, C. Wang, X. Qu, *Nat. Commun.* **2019**, *10*, 2695.
[227] Z. L. Wang, J. Chen, L. Lin, *Energy Environ. Sci.* **2015**, *8*, 2250.
[228] U. Khan, R. Hinchet, H. Ryu, S. W. Kim, *APL Mater.* **2017**, *5*, 073803.
[229] J. Wang, S. Li, F. Yi, Y. Zi, J. Lin, X. Wang, Y. Xu, Z. L. Wang, *Nat. Commun.* **2016**, *7*, 12744.
[230] H. Guo, M. H. Yeh, Y. C. Lai, Y. Zi, C. Wu, Z. Wen, C. Hu, Z. L. Wang, *ACS Nano* **2016**, *10*, 10580.
[231] X. Pu, L. Li, M. Liu, C. Jiang, C. Du, Z. Zhao, W. Hu, Z. L. Wang, *Adv. Mater.* **2016**, *28*, 98.
[232] J. Luo, F. R. Fan, T. Jiang, Z. Wang, W. Tang, C. Zhang, M. Liu, G. Cao, Z. L. Wang, *Nano Res.* **2015**, *8*, 3934.
[233] S. Jung, J. Lee, T. Hyeon, M. Lee, D. H. Kim, *Adv. Mater.* **2014**, *26*, 6329.
[234] X. Wang, Y. Yin, F. Yi, K. Dai, S. Niu, Y. Han, Y. Zhang, Z. You, *Nano Energy* **2017**, *39*, 429.
[235] Q. Jiang, C. Wu, Z. Wang, A. C. Wang, J. H. He, Z. L. Wang, H. N. Alshareef, *Nano Energy* **2018**, *45*, 266.
[236] K. Dong, Y. C. Wang, J. Deng, Y. Dai, S. L. Zhang, H. Zou, B. Gu, B. Sun, Z. L. Wang, *ACS Nano* **2017**, *11*, 9490.
[237] S. Hong, J. Lee, K. Do, M. Lee, J. H. Kim, S. Lee, D. H. Kim, *Adv. Funct. Mater.* **2017**, *27*, 1704353.
[238] J. Chen, H. Guo, X. Pu, X. Wang, Y. Xi, C. Hu, *Nano Energy* **2018**, *50*, 536.
[239] A. Ramadoss, B. Saravanakumar, S. W. Lee, Y. S. Kim, S. J. Kim, Z. L. Wang, *ACS Nano* **2015**, *9*, 4337.
[240] N. Wang, W. Dou, S. Hao, Y. Cheng, D. Zhou, X. Huang, C. Jiang, X. Cao, *Nano Energy* **2019**, *56*, 868.
[241] R. Song, H. Jin, X. Li, L. Fei, Y. Zhao, H. Huang, H. L. W. Chan, Y. Wang, Y. Chai, *J. Mater. Chem. A* **2015**, *3*, 14963.
[242] Z. He, B. Gao, T. Li, J. Liao, B. Liu, X. Liu, C. Wang, Z. Feng, Z. Gu, *ACS Sustainable Chem. Eng.* **2019**, *7*, 1745.
[243] A. Maitra, S. K. Karan, S. Paria, A. K. Das, R. Bera, L. Halder, S. K. Si, A. Bera, B. B. Khatua, *Nano Energy* **2017**, *40*, 633.
[244] C. Li, M. M. Islam, J. Moore, J. Sleppy, C. Morrison, K. Konstantinov, S. X. Dou, C. Renduchintala, J. Thomas, *Nat. Commun.* **2016**, *7*, 13319.
[245] T. Chen, L. Qiu, Z. Yang, Z. Cai, J. Ren, H. Li, H. Lin, X. Sun, H. Peng, *Angew. Chem., Int. Ed.* **2012**, *51*, 11977.
[246] P. Sun, M. Qiu, M. Li, W. Mai, G. Cui, Y. Tong, *Nano Energy* **2019**, *55*, 506.
[247] Z. Chai, N. Zhang, P. Sun, Y. Huang, C. Zhao, H. J. Fan, X. Fan, W. Mai, *ACS Nano* **2016**, *10*, 9201.
[248] Z. Wen, M. H. Yeh, H. Guo, J. Wang, Y. Zi, W. Xu, J. Deng, L. Zhu, X. Wang, C. Hu, *Sci. Adv.* **2016**, *2*, e1600097.
[249] R. A. Alshehhi, M. S. Arefin, T. Wu, M. R. Yuce, in *Proc. 11th EAI Int. Conf. Body Area Networks*, ICST (Institute for Computer Sciences, Social-Informatics and Telecommunications Engineering), Turin, Italy, December **2016**.
[250] M. Wahbah, M. Alhawari, B. Mohammad, H. Saleh, M. Ismail, *IEEE J. Emerging Sel. Top. Circuits Syst.* **2014**, *4*, 354.
[251] F. Deng, H. Qiu, J. Chen, L. Wang, B. Wang, *IEEE Trans. Ind. Electron.* **2016**, *64*, 1477.
[252] V. Leonov, R. J. M. Vullers, *J. Renewable Sustainable Energy* **2009**, *1*, 062701.
[253] V. Leonov, C. Van Hoof, R. J. M. Vullers, *Sixth International Workshop on Wearable and Implantable Body Sensor Networks*, Berkeley, USA **2009**.
[254] S. Y. Heo, J. Kim, P. Gutruf, A. Banks, P. Wei, R. Pielak, G. Balooch, Y. Shi, H. Araki, D. Rollo, *Sci. Transl. Med.* **2018**, *10*, eaau1643.
[255] Y. Yue, Z. Yang, N. Liu, W. Liu, H. Zhang, Y. Ma, C. Yang, J. Su, L. Li, F. Long, *ACS Nano* **2016**, *10*, 11249.
[256] D. Kim, D. Kim, H. Lee, Y. R. Jeong, S. J. Lee, G. Yang, H. Kim, G. Lee, S. Jeon, G. Zi, *Adv. Mater.* **2016**, *28*, 748.
[257] X. Cao, A. Halder, Y. Tang, C. Hou, H. Wang, J. Ø. Duus, Q. Chi, *Mater. Chem. Front.* **2018**, *2*, 1944.
[258] W. Gao, S. Emaminejad, H. Y. Y. Nyein, S. Challa, K. Chen, A. Peck, H. M. Fahad, H. Ota, H. Shiraki, D. Kiriya, *Nature* **2016**, *529*, 509.
[259] Y. R. Jeong, G. Lee, H. Park, J. S. Ha, *Acc. Chem. Res.* **2019**, *52*, 91.
[260] T. R. Ray, J. Choi, A. J. Bandodkar, S. Krishnan, P. Gutruf, L. Tian, R. Ghaffari, J. A. Rogers, *Chem. Rev.* **2019**, *119*, 5461.
[261] Y. Chen, B. Xu, J. Gong, J. Wen, T. Hua, C. W. Kan, J. Deng, *ACS Appl. Mater. Interfaces* **2019**, *11*, 2120.
[262] S. Chun, W. Son, G. Lee, S. H. Kim, J. W. Park, S. J. Kim, C. Pang, C. Choi, *ACS Appl. Mater. Interfaces* **2019**, *11*, 9301.
[263] J. Zhao, Y. Zhang, Y. Huang, J. Xie, X. Zhao, C. Li, J. Qu, Q. Zhang, J. Sun, B. He, *Adv. Sci.* **2018**, *5*, 1801114.
[264] W. Li, X. Xu, C. Liu, M. C. Tekell, J. Ning, J. Guo, J. Zhang, D. Fan, *Adv. Funct. Mater.* **2017**, *27*, 1702738.
[265] Y. Song, H. Chen, X. Chen, H. Wu, H. Guo, X. Cheng, B. Meng, H. Zhang, *Nano Energy* **2018**, *53*, 189.
[266] J. Yun, C. Song, H. Lee, H. Park, Y. R. Jeong, J. W. Kim, S. W. Jin, S. Y. Oh, L. Sun, G. Zi, *Nano Energy* **2018**, *49*, 644.
[267] L. Yu, Y. Yi, T. Yao, Y. Song, Y. Chen, Q. Li, Z. Xia, N. Wei, Z. Tian, B. Nie, *Nano Res.* **2019**, *12*, 331.
[268] L. Li, C. Fu, Z. Lou, S. Chen, W. Han, K. Jiang, D. Chen, G. Shen, *Nano Energy* **2017**, *41*, 261.
[269] B. U. Hwang, J. H. Lee, T. Q. Trung, E. Roh, D. I. Kim, S. W. Kim, N. E. Lee, *ACS Nano* **2015**, *9*, 8801.
[270] X. Liang, G. Long, C. Fu, M. Pang, Y. Xi, J. Li, W. Han, G. Wei, Y. Ji, *Chem. Eng. J.* **2018**, *345*, 186.
[271] Y. Song, H. Chen, Z. Su, X. Chen, L. Miao, J. Zhang, X. Cheng, H. Zhang, *Small* **2017**, *13*, 1702091.
[272] H. Park, J. W. Kim, S. Y. Hong, G. Lee, D. S. Kim, J. h. Oh, S. W. Jin, Y. R. Jeong, S. Y. Oh, J. Y. Yun, *Adv. Funct. Mater.* **2018**, *28*, 1707013.
[273] Y. Lu, K. Jiang, D. Chen, G. Shen, *Nano Energy* **2019**, *58*, 624.
[274] Y. Lin, J. Chen, M. M. Tavakoli, Y. Gao, Y. Zhu, D. Zhang, M. Kam, Z. He, Z. Fan, *Adv. Mater.* **2019**, *31*, 1804285.
[275] R. Guo, J. Chen, B. Yang, L. Liu, L. Su, B. Shen, X. Yan, *Adv. Funct. Mater.* **2017**, *27*, 1702394.
[276] Y. Ai, Z. Lou, S. Chen, D. Chen, Z. M. Wang, K. Jiang, G. Shen, *Nano Energy* **2017**, *35*, 121.
[277] J. Koo, M. R. MacEwan, S. K. Kang, S. M. Won, M. Stephen, P. Gamble, Z. Xie, Y. Yan, Y. Y. Chen, J. Shin, *Nat. Med.* **2018**, *24*, 1830.
[278] H. Li, C. Zhao, X. Wang, J. Meng, Y. Zou, S. Noreen, L. Zhao, Z. Liu, H. Ouyang, P. Tan, *Adv. Sci.* **2019**, *6*, 1801625.